ESS2222H

Tectonics and Planetary Dynamics
Lecture 9
Iron Spin Transition in the Lower Mantle

Hosein Shahnas

University of Toronto, Department of Earth Sciences,

The Spin States of Iron in Earth's Lower Mantle

Fundamentals

Spin Paring

Pressure-induced **spin paring transitions** of iron were **predicted** about 60 years ago **(Fyfe, 1960)** and **recently** have been **detected** in lower mantle pressures (e.g. Badro et al., 2003, 2004, 2005; Li et. al, 2004; Lin et. al, 2005, 2007, 2008).

As **pressure** increases, **iron** in **Perovskite** and **Magnesiowustite** transforms gradually from the initial **high-spin** state (with high number of unpaired electrons) toward the final **low-spin** state (with low number of unpaired electrons**)** (Sherman, 1991; Li et al., 2004; Tsuchiya et al., 2004, 2006; Lin et al., 2008; Goncharov,et al. 2006; McCammon et al., 2008).

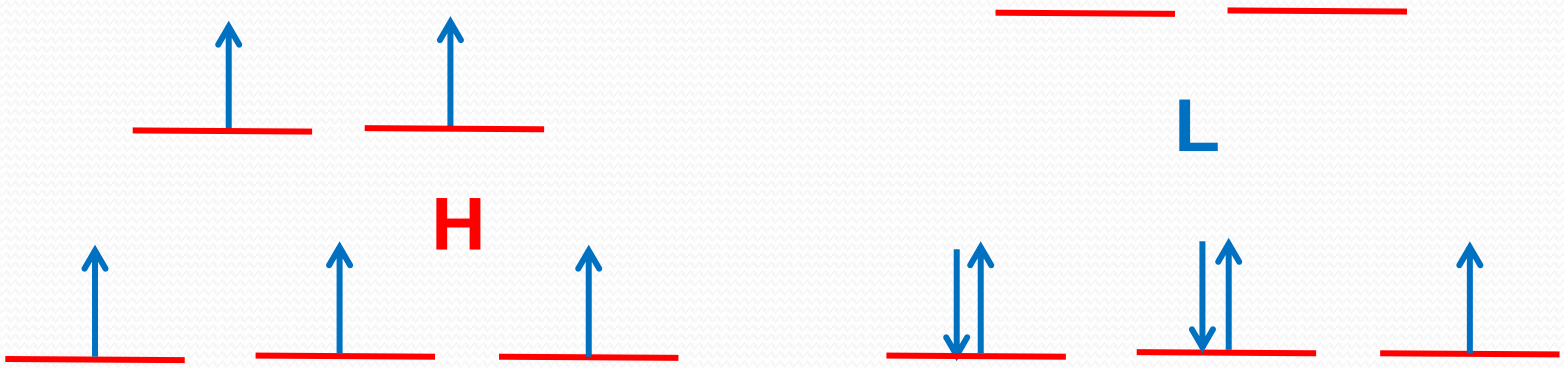

Fundamentals

Aufbau Principle

In the ground state of an atom electrons fill atomic orbitals of the lowest available energy levels before occupying higher levels.

Hund's Rule

If multiple orbitals of the **same energy** are available, electrons will occupy different orbitals **singly** before any are occupied doubly.

Electron Configuration

Subshells →
Shells ↓

1s
2s 2p
3s 3p 3d
4s 4p 4d 4f
5s 5p 5d 5f 5g
6s 6p 6d 6f 6g …
7s 7p 7d 7f 7g …
8s 8p 8d 8f 8g …

2 6 10 14 18 …

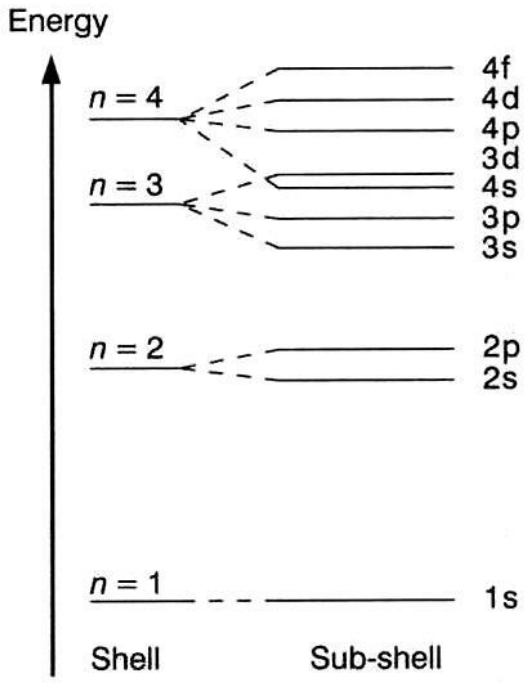

1s, 2s, 2p, 3s, 3p, 4s, 3d, 4p, 5s, 4d, 5p, 6s, 4f, 5d, 6p, 7s, 5f, 6d, 7p, 8s, 5g, …

Fundamentals

The Pauli Exclusion Principle

Two or more identical fermions (particles with half-integer spin) **cannot occupy** the **same quantum state** within a quantum system simultaneously.

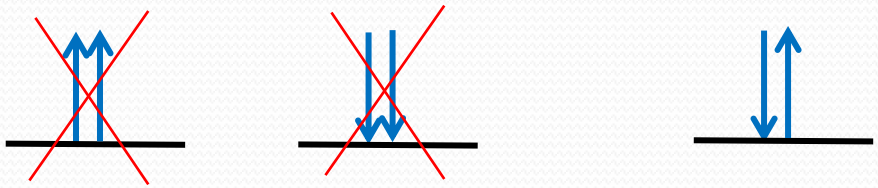

The **maximum number of electrons** in any **shell** = $2n^2$ *n: principal quantum number*

The maximum number of electrons in a subshell (s, p, d or f) is equal to $2(2\ell+1)$ where $\ell = 0, 1, 2, 3$

Fundamentals

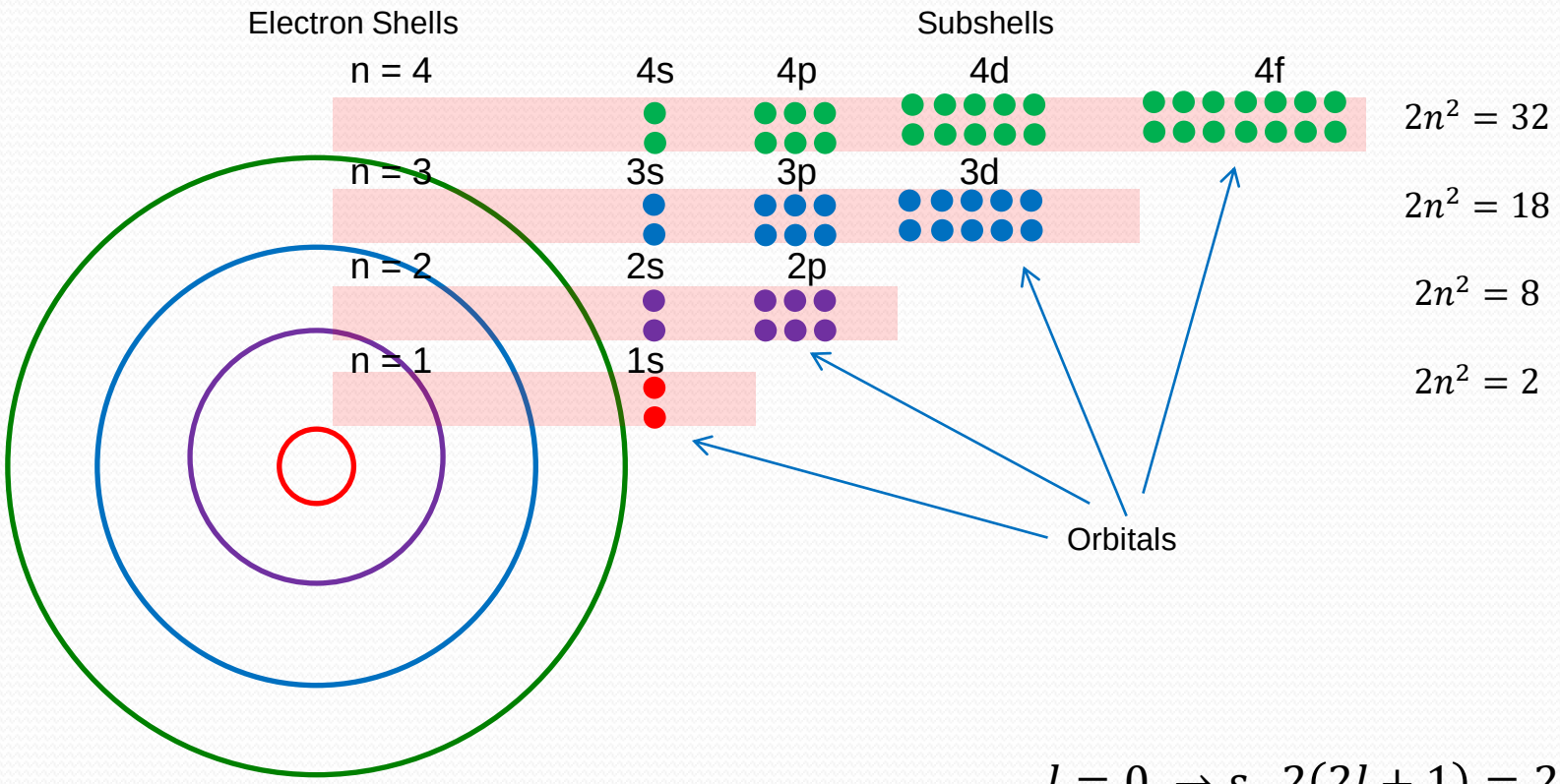

$2n^2 = 32$

$2n^2 = 18$

$2n^2 = 8$

$2n^2 = 2$

n = 1: K
n = 2: L
n = 3: M
… … …

$l = 0 \rightarrow s \quad 2(2l+1) = 2$
$l = 1 \rightarrow p \quad 2(2l+1) = 6$
$l = 2 \rightarrow d \quad 2(2l+1) = 10$
$l = 3 \rightarrow f \quad 2(2l+1) = 14$
$l = 4 \rightarrow g \quad 2(2l+1) = 18$

General Rules to Predict Electronic Configurations

a) Electrons are assigned to orbitals in order of **increasing** value of **(n+ℓ).**
b) For subshells with the **same** value of **(n+ℓ),** electrons are assigned first to the sub shell with **lower *n*.**

1s,	2s,	2p,	3s,	3p,	4s,	3d,	4p,	5s,	4d,	5p,	6s,	4f,	5d,	6p,	7s,	5f,	6d,	7p,	8s,	5g,	
1,	2,	2,	3,	3,	4,	3,	4,	5,	4,	5,	6,	4,	5,	6,	7,	5,	6,	7,	8,	5	**n**
0,	0,	1,	0,	1,	0,	2,	1,	0,	2,	1,	0,	3,	2,	1,	0,	3,	2,	1,	0,	4,	**ℓ**
1,	2,	3,	3,	4,	4,	5,	5,	5,	6,	6,	6,	7,	7,	7,	7,	8,	8,	8,	8,	9,	**n+ℓ**
2,	2,	6,	2,	6,	2,	10,	6,	2,	10,	6,	2,	14,	10,	6,	2,	14,	10,	6,	2,	18,	**2(2ℓ+1)**

Fe: [Ar] $3d^6\ 4S^2$
z = 18 + 6 + 2

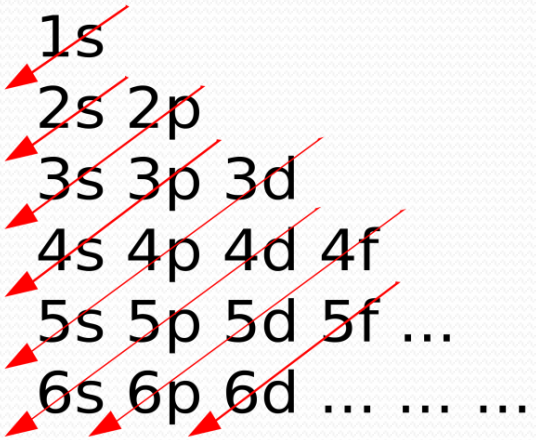

Transition Metals

The **columns (groups),** contain elements with similar **chemical** behaviours.
The **rows (periods),** generally have **metals** on the **left** and **non-metals** on the **right**.

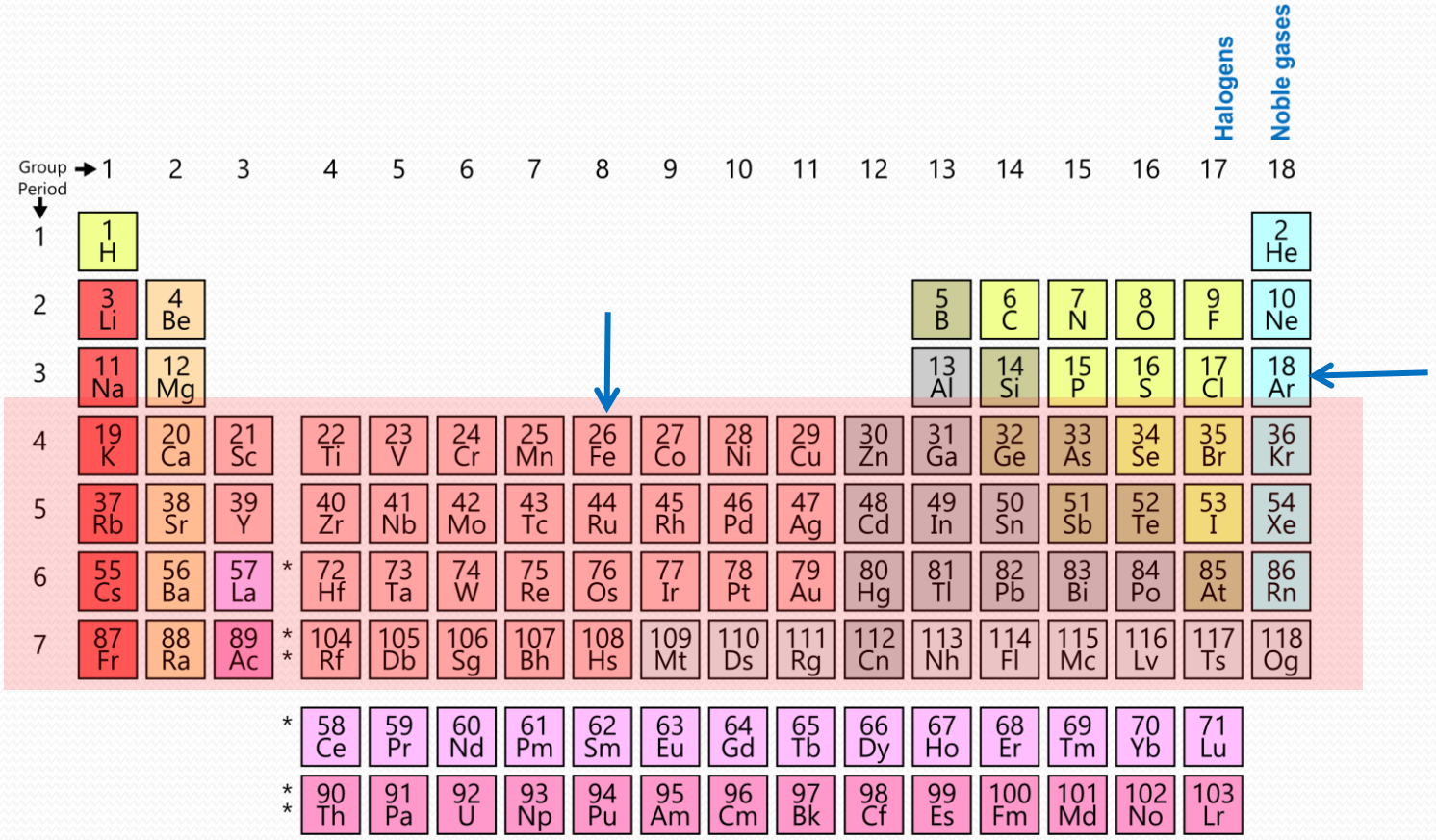

https://commons.wikimedia.org/w/index.php?curid=62296883

Transition Metals

Transition metals or d-block elements?

They are often used **interchangeably** but they are **not the same**. Not all d-block elements count as transition metals.

A **transition metal** is one which forms **one or more stable ions** with **incompletely** filled **d-orbitals.**

Iron is **3d-transition metal** (incomplete d-orbitals), with high **density**, high **melting point**, **paramagnetic**, **variable oxidation states**. Transition metals have

a) **Low ionization energies**
b) **Multiple oxidation states**, since there is a low energy gap between the states

Fe : [Ar] $3d^6\ 4S^2$

Fe^{2+} : [Ar] $3d^6$

Fe^{3+} : [Ar] $3d^5$

Transition Metals

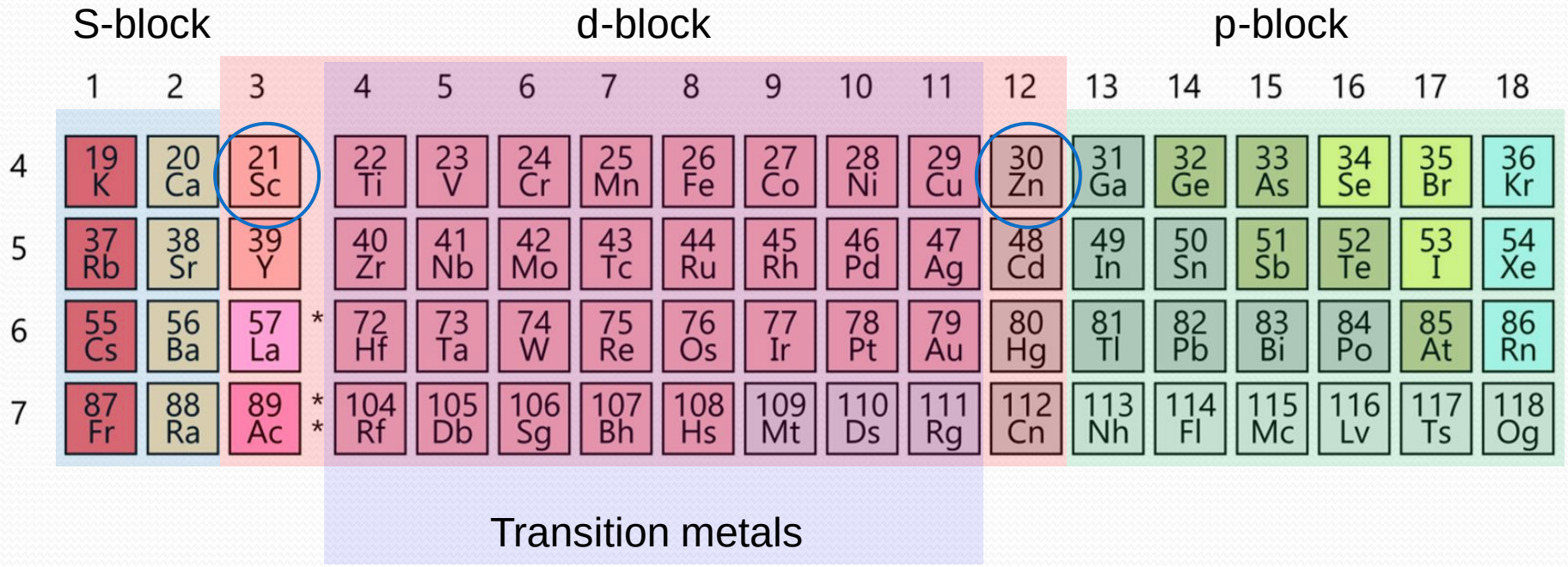

Ex. - Scandium and **Zinc** are **d-block** metal but **not transition metal** (because in their ions there is no incomplete d-orbital, or d-orbital is missing).

Sc: [Ar] $3d^1 4s^2$ → Sc^{3+}: [Ar]

Zn: [Ar] $3d^{10} 4s^2$ → Zn^{2+}: [Ar] $3d^{10}$

The Spin States of Iron in Earth's Lower Mantle

Early Theoretical Prediction

It has been suggested theoretically (Shermann, 1991) that iron in **ferropericlase** undergoes a **high spin (HS)** to **low spin (LS)** transition in the pressure domain of the lower mantle, **while iron** in **perovskite remains** in **HS** phase at the same pressure conditions (Cohen et al., 1997).

Most Recent Studies

Fe^{2+}- iron in $MgSiO_3$-Pv is **less likely** to make transition to **LS**

Fe^{3+}- iron in $MgSiO_3$-Pv occupies both **A** and **B** sites (with equal weighting)

A remains in **HS** in all mantle pressures

B → Fully **LS** in the range of 50-60 GPa

Catalli et al. (2009, 2010, 2011)

The Spin States of Iron in Earth's Lower Mantle

Crystal Field Theory

Crystal field theory (CFT) describes the **breaking** of **orbital degeneracy** in **transition metal** complexes **due to the presence of ligands**. CFT qualitatively describes the strength of the metal-ligand bonds. Based on **the strength of the metal-ligand bonds**, the energy of the **system is altered**. → This may lead to a **change** in **magnetic properties** as well as color and other properties. This theory was developed by Hans Bethe and John Hasbrouck van Vleck.

The theory describes the energy changes of the **five degenerate d- orbitals** being surrounded by an array of point charges consisting of the **ligands** (any atom or molecule attached to a central atom, usually a metallic element). The basis of the model is the **interaction** of **d-orbitals** of a central atom with **ligands**, which are considered as point charges.

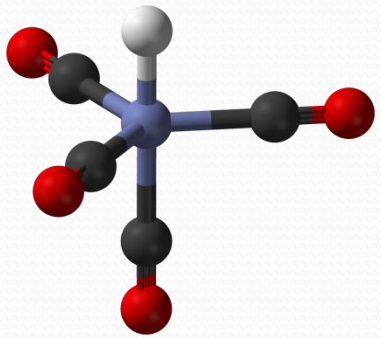

The Spin States of Iron in Earth's Lower Mantle

Field Splitting by Ligands

The **d-electrons** closer to the ligands will have a higher energy than those further away, which results in the d-orbitals splitting in energy.

Δ: Crystal field stabilization parameter (energy splitting)

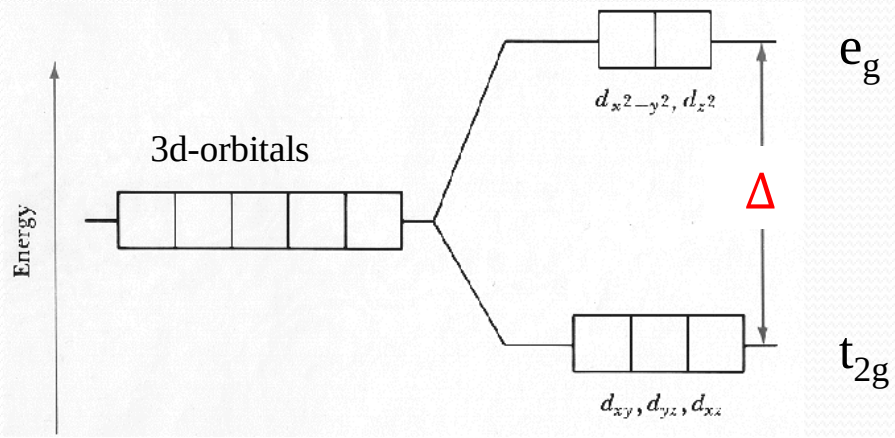

The Spin States of Iron in Earth's Lower Mantle

HS-LS Spin Transition

As pressure increase in mantle by depth, the bond distance between iron and oxygen decreases. The splitting Δ parameter is proportional to the **inverse** of the Fe-O **bond distance.** However the **pairing** energy **does not** change much by **pressure**.

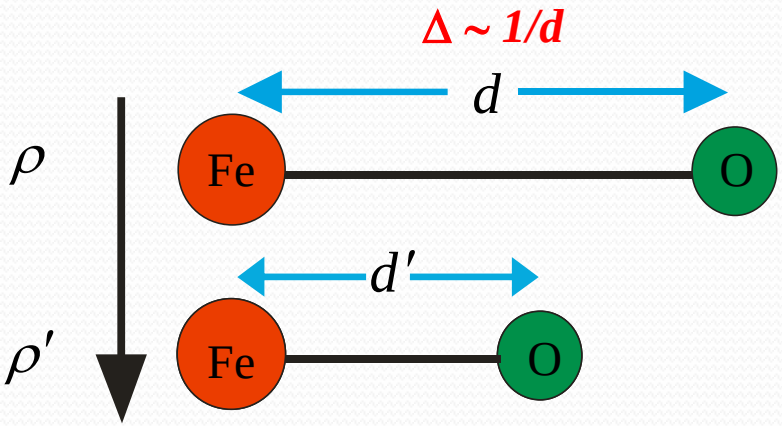

Weak-field: $\frac{E_p}{\Delta}\uparrow$ → **HS**

Strong-field: $\frac{E_p}{\Delta}\downarrow$ → **LS**

Depth increasing

$pressure\uparrow$ → $\rho' > \rho$, $d' < d$, $E'_p \approx E_p$ → $\Delta' > \Delta$ → $\frac{E'_p}{\Delta'} < \frac{E_p}{\Delta}$ → $HS \Rightarrow LS$

The Spin States of Iron in Earth's Lower Mantle

Because of the **splitting** in the energy level of **d-orbital,** the electrons may settle in the **lower** energy level t_{2g} or in the **higher** level e_g.

Depending on E_p (paring energy) and Δ (crystal field stabilization parameter) the lowest energy configuration could either be in **LS** state or **HS** state.

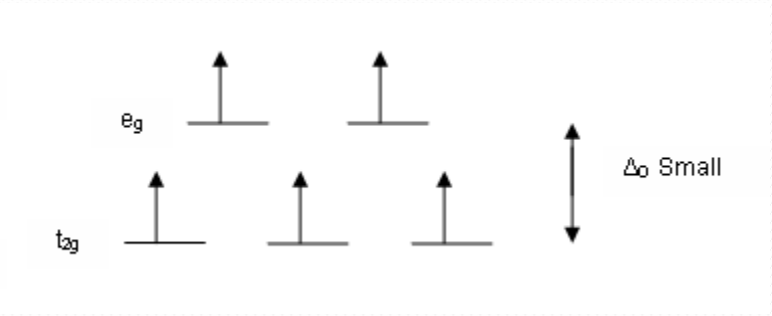

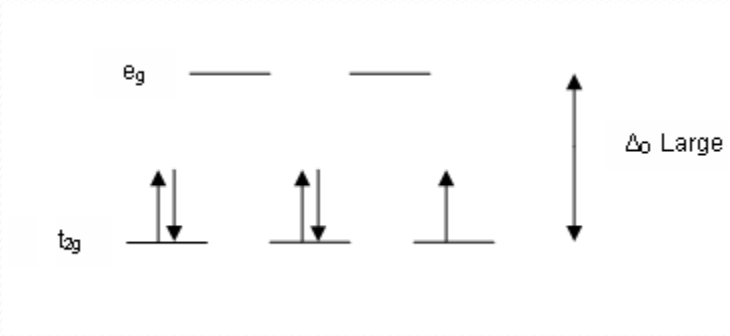

For **small** Δ the electrons have **a chance** to jump to the higher energy level e_g
For **large** Δ the electrons have **less chance** to jump to the higher energy level e_g

X-Ray Emission Spectroscopy (XES)

XES

X-ray emission spectroscopy (XES) is one of the so-called photon-in - photon-out spectroscopies in which a core electron is excited by an incident x-ray photon and then this excited state decays by emitting an x-ray photon to fill the core hole. X-ray emission spectroscopy (XES) is a spectroscopic technique for probing the structure of the low-energy outer most electronic levels of chemical elements (Jenkins, 1999).

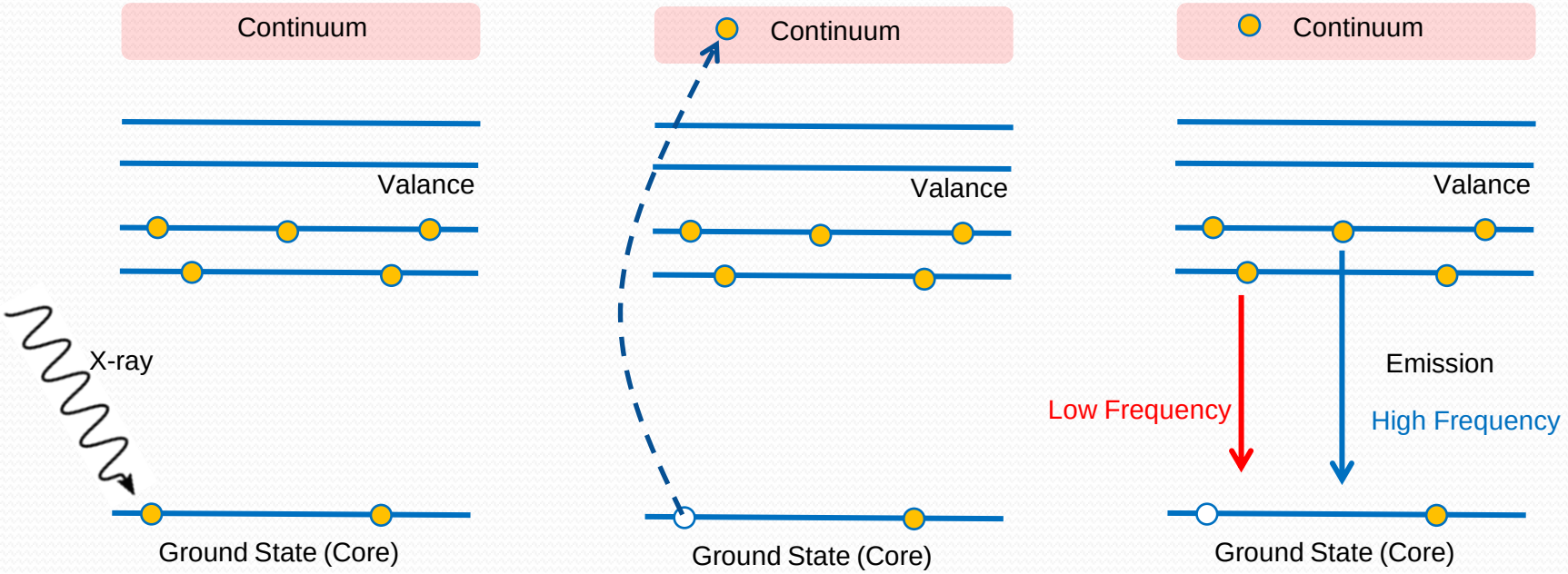

X-Ray Emission Spectroscopy (XES)

$K\alpha$ Emission

$K\alpha$ Emission lines result when an electron transitions to a vacancy in the innermost "K" shell (principal quantum number n = 1) from a **2p-orbital** of the second, **L-shell** (n = 2), leaving a vacancy there.

$K\beta$ Emission

$K\beta$ emissions, similar to $K\alpha$ emissions, result when an electron transitions to the innermost "K" shell (principal quantum number 1) from a **3p-orbital** of the third or **M-shell** (with principal quantum number 3).

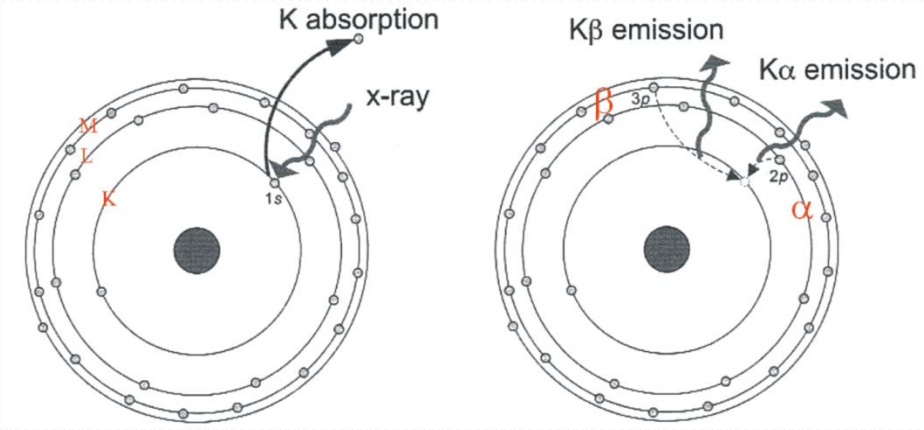

Photoelectric Effect — X-Ray Fluorescence

x-ray absorption — K_α and K_β emissions

The shell structure of Fe $^{2+}$ ion (Badro et al., 2005)

X-Ray Emission Spectroscopy (XES)

The **hole** in **3p** shell strongly interacts with the magnetic moment of **3d** shell, allowing determination of 3d shell. As pressure increases **HS** → **LS** (the low energy **Satellite** disappears)

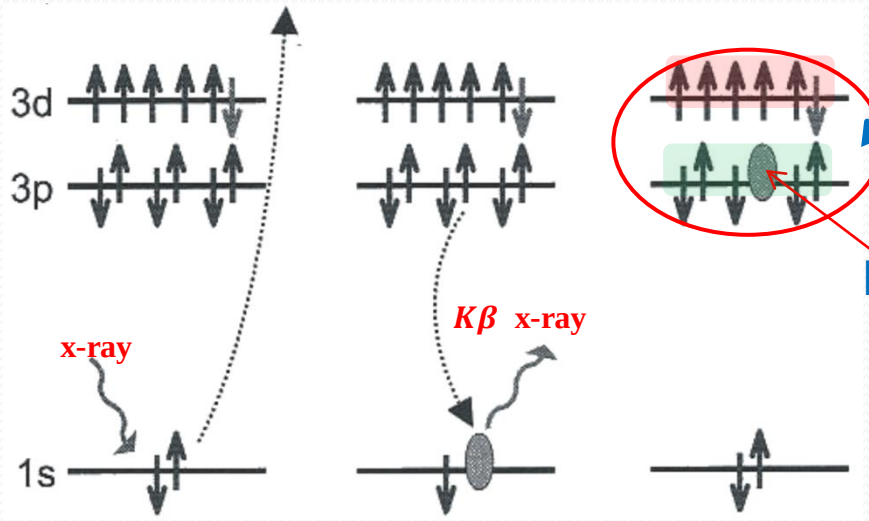

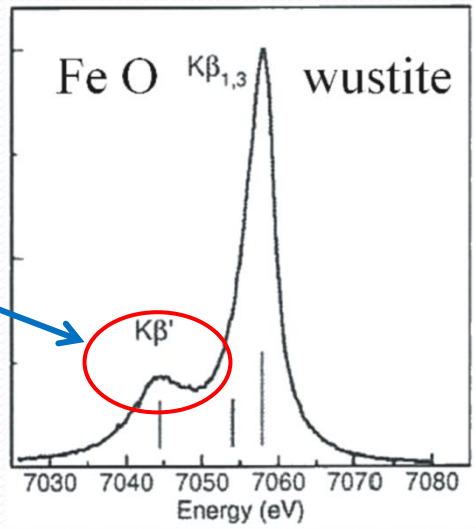

x-ray absorption **Kβ x-ray emission**

Iron Spin Transition in Perovskite

$K\beta$ emissions result when an electron transitions to the innermost K shell (n = 1) from a **3p** orbital of the third or M shell (n = 3).

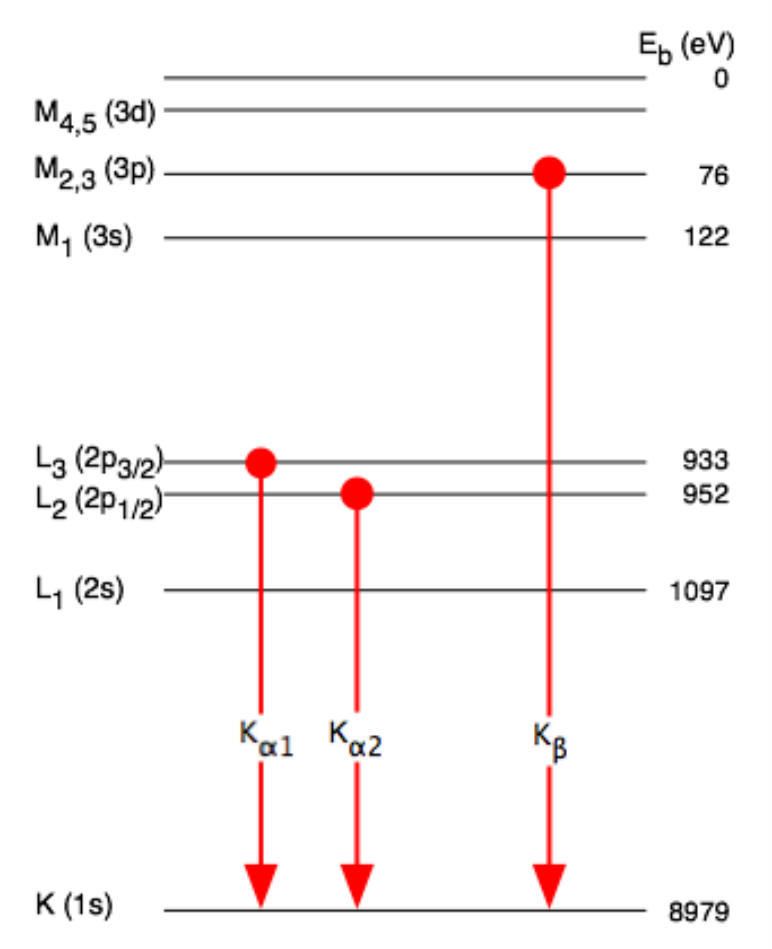

Iron Spin Transition in Ferropericlase

Iron Spin Transition in Ferropericlase

Experimental Evidence - I

The eventual collapse of the 3*d* magnetic moment as a consequence of pressure increase should lead to the disappearance of the low energy **satellite**, a very clear spectral signature (Badro et al., 1999).

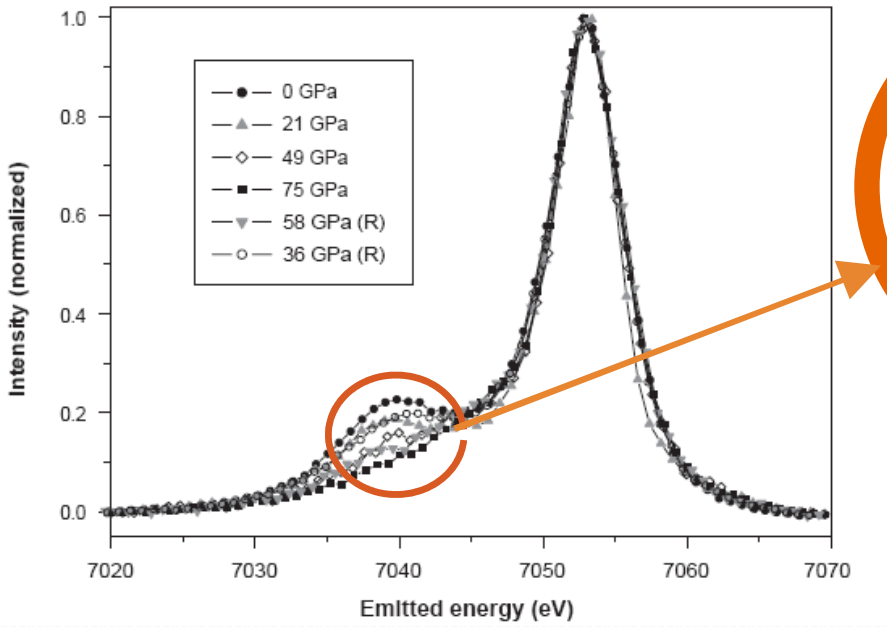

~ **High spin population**

In LS state total magnetic moment → 0

X-ray emission spectra collected on ferropericlase **$(Mg_{0.83}Fe_{0.17})O$** at different pressures. The system is in the **HS state at 36 GPa,** in a **HS-LS mixture at 49** and 58 GPa, and in the **LS state at 75 GPa.** The pure LS component appears between 58 and 75 Gpa (Badro et al., 2003).

Iron Spin Transition in Ferropericlase

Experimental Evidence - II

The experimental work of J.F. Lin et. Al (2007) on ferropericlase **[$(Mg_{0.75},Fe_{0.25})O$]** at pressure and temperature up to **95 GPa and 2000 K** respectively, shows a gradual spin transition of iron from **~1000 km depth** and 1900 K to 2200 km and 2300 K.

Note that:

Ferropericlase [$(Mg_{1-x}Fe_x)O$, $x <= 0.5$],

Magnesiowustite : [$(Mg_{1-x}Fe_x)O$, $x > 0.5$]

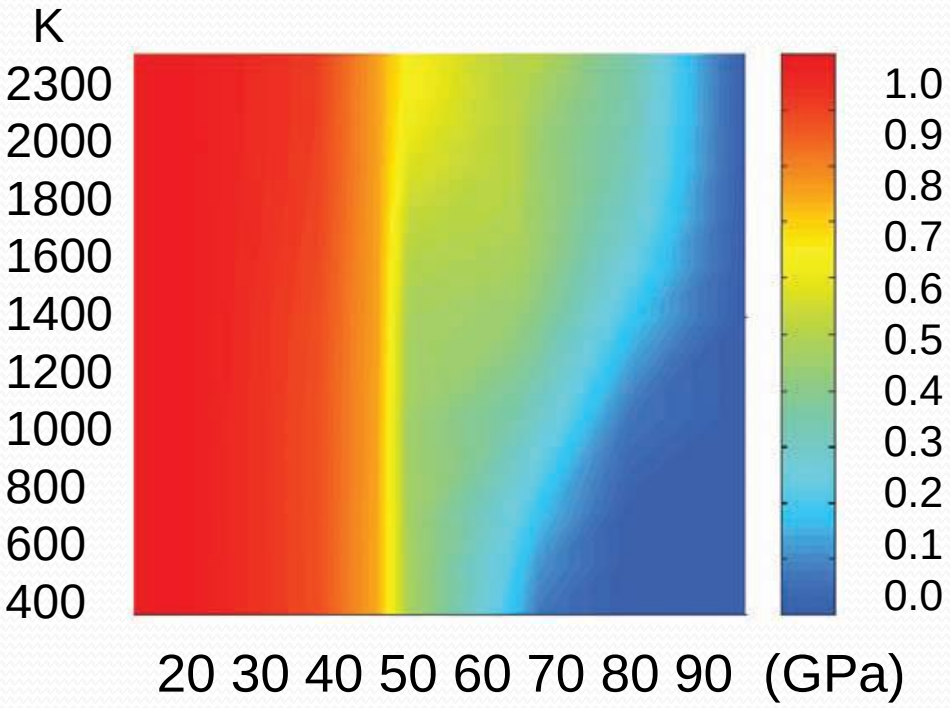

Spin transition of Fe2+ in $(Mg_{0.75},Fe_{0.25})O$. Colors in the vertical column on the right represent fractions of the high-spin iron, in $(Mg_{0.75},Fe_{0.25})O$ (Lin et. al, 2007).

Iron Spin Transition in Ferropericlase

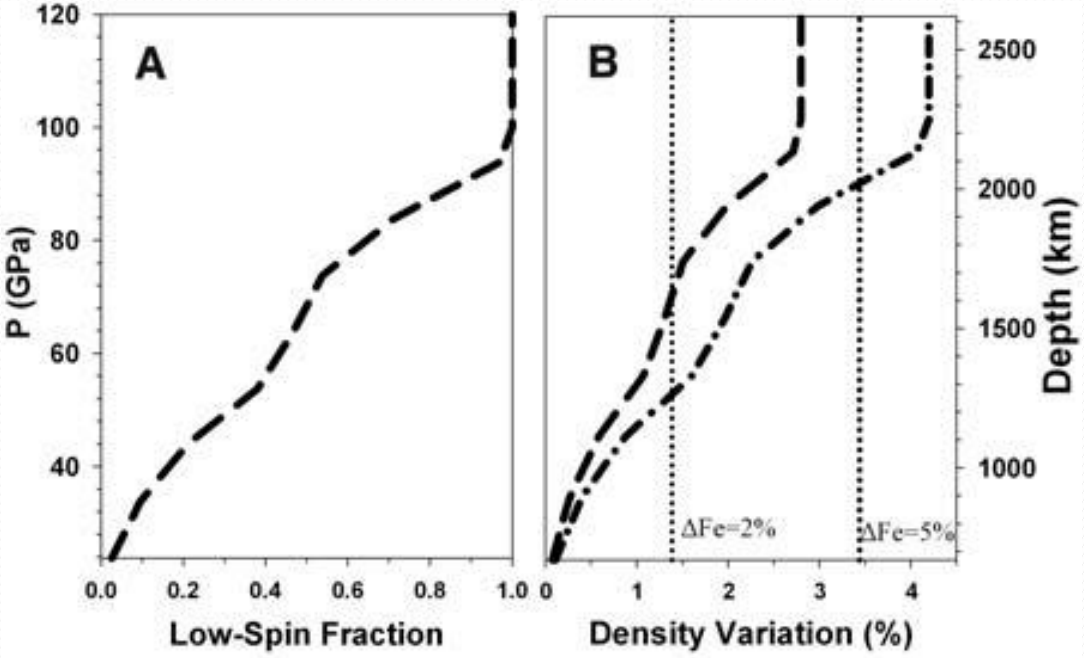

A) Derived fractions of the low-spin ferropericlase and B) density variation along a model lower-mantle geotherm. Density variations in ferropericlase across the spin crossover region assume a linear dependence of the density on the fraction of the low-spin iron. Dashed line and dash-dotted line represent derived density variations using maximum variations of 2.8% and 4.2% across the spin-crossover region respectively.

Iron Spin Transition in Perovskite

Iron Spin Transition in Perovskite

Experimental Evidence - III

(A) X-ray emission spectra collected on **$(Mg_{0.9},Fe_{0.1})SiO_3$** between **20** and **145** GPa. The presence of a **satellite structure ($K\beta'$ line)** on the low-energy side of the iron main emission ($K\beta_{13}$) line is **characteristic of a HS 3*d* magnetic moment.** The spin state of iron transforms twice at **70 and 120 GPa,** as indicated by the changes in K line intensity. Moreover, the position of the **$K\beta_{13}$** line shifts with each transition (central position shown by the vertical dashed lines) and by a total of –0.75 eV between 20 and 145 GPa, which is in agreement with a HS-LS transition in iron.

(B) The **solid lines** are **models** constructed from reference molecular compounds and are not fitted to the data. **Three spectra** taken from three different states (HS at 20 GPa, mixed state at 100 GPa, and LS at 145 GPa) are plotted on top to show the agreement. Bardo et. Al (2005)

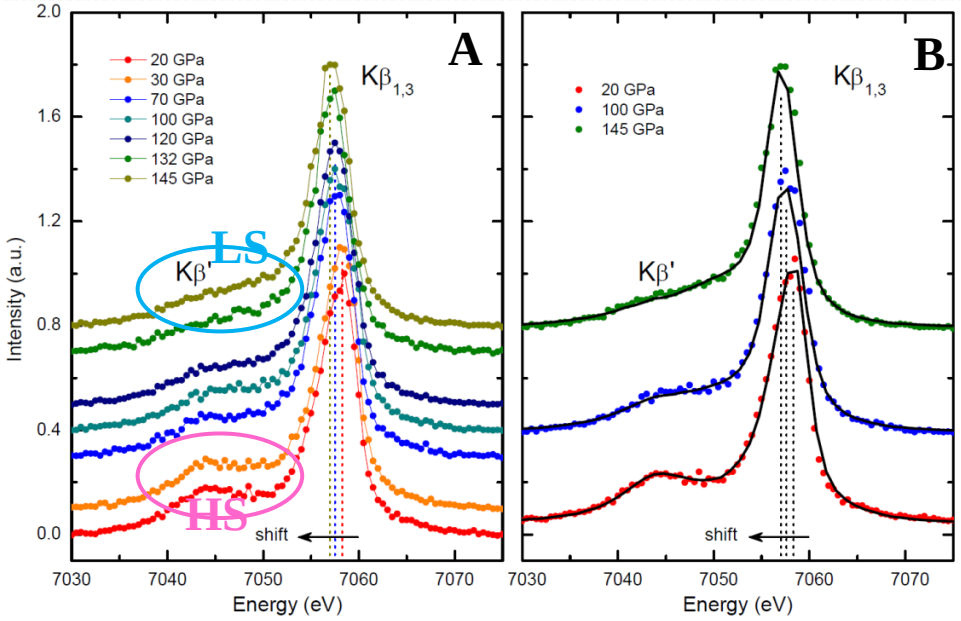

Iron Spin Transition in Perovskite

The experimental work of Bardo et. Al (2005) on Perovskite **[$(Mg_{0.9},Fe_{0.1})SiO_3$]** at **70 Gpa** and at **120 Gpa**, corresponding to **partial** and **full** electron pairing in iron, respectively.

The system evolves in **three** independent states: the **HS state** below 70 GPa, the **mixed state** between 70 and 120 GPa, and the **LS state** above 120 GPa.

(**A**) Average quantum spin number on the iron atom as a function of pressure, derived from the intensity of the $K\beta'$ line indicating two transitions in perovskite at 70 and 120 GPa (1700 and 2600 km depths rep.). In the mixed state, the two curves represent upper and lower bounds of the iron magnetic moment.

B) $K\beta_{13}$ line position **(central shift)** as a function of pressure, showing again that the two transitions occur at 70 and 120 GPa.

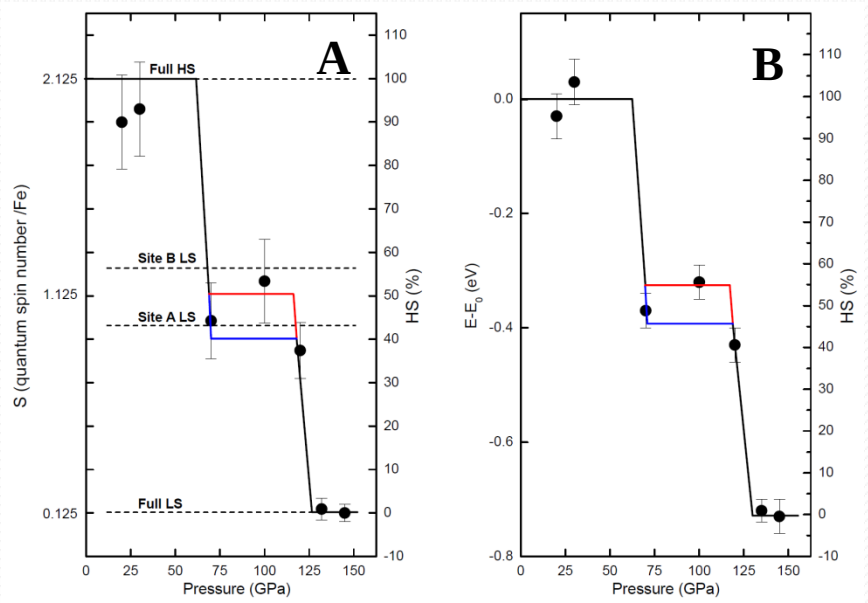

The Influence of Iron Spin Transition in Mantle Properties

Impacts of Iron Spin Transition

The main constituents of the Earth's lower mantle

Iron-bearing magnesium **silicate perovskite**, $(Mg,Fe)SiO_3$ *(the most abundant phase)*
Magnesiowustite, (Mg,Fe)O

Both these minerals undergo **high spin (HS)** to **low spin (LS)** as pressure increases with depth.

Impacts on the Vigour of Convection in D"-layer

Heat produced from the **secular cooling** of the core and **radioactive** decay can be transported in the mantle by a) **conduction**, b) **radiation**, or c) **convection**.
Convection is **only initiated** if the other two processes **fail** to transfer the heat

Iron spin transition can **influence** the **radiation** and **conduction** properties of the mantle material and hence the **convection**. It also influence the other properties as **thermal expansivity, density, viscosity**, and the **bulk modulus** which all influence mantle convection.

Impacts of Iron Spin Transition

Impact of spin transition on partition coefficient of iron

A HS-LS spin transition occurs the 60-70-GP pressure range (~2000 km depths). This transition implies that the **partition coefficient** of iron between ferropericlase and magnesium silicate perovskite, the two main constituents of the lower mantle, **may increase** by several orders of magnitude, **depleting the perovskite phase of its iron**. The lower mantle may then be composed of two different layers. The upper layer would consist of a phase mixture with about equal partitioning of iron between magnesium silicate perovskite and ferropericlase, **whereas the lower layer would consist of almost iron-free perovskite and iron-rich ferropericlase** (Badro et. al, 2003).

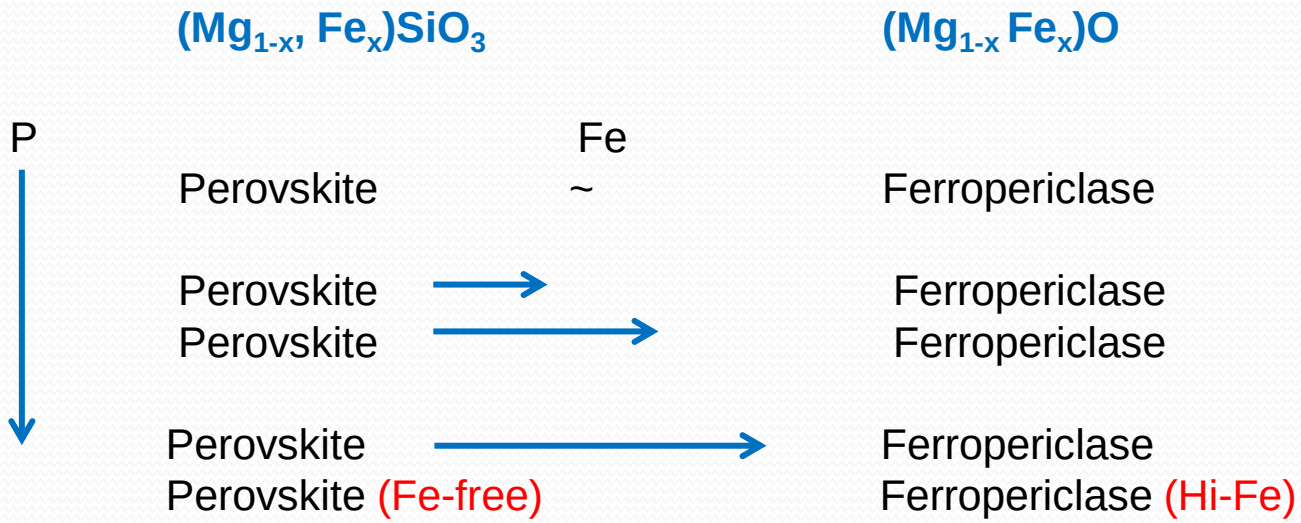

Impacts of Iron Spin Transition

A Transition Toward the Low-Spin State

1- As **perovskite** or **magnesiowustite** makes transition from **HS** to **LS**, the **absorption bands** initially in the **infrared (IR) and red** region shift to the **green-blue-Violet** region. This is called a **blue shift** of the absorption bands (Burns, 1993; Sherman, 1991). As a result the **transparency** of these minerals in the **infrared region** increases with depth with in D" layer. The resulting **increase** in **radiative** thermal conductivity would decrease the **vigour** of convection in the lowermost mantle

2- The **number of unpaired electrons** is **decreased** in the **3d-subshell** of iron (Burns, 1993). This leads to a decrease in the **magnetic susceptibility** of its host phase appreciable effects on the **magnetic properties** of the lower mantle material (perovskite).

3- The **ionic radius** becomes smaller than its high-spin counterpart (Shannon, 1963).

4- (2) and (3) affect the **thermoelastic** properties of the host phases (Sherman, 1988).

Impacts of Iron Spin Transition

5- More importantly, it would significantly modify the **chemical bonding** character of Fe^{2-} and Fe^{3-} ions (Burns, 1993; Cohen, 1997).

6- It can also **increase partial melting** (Gaffney and Anderson, 1973; Keken et al., 1995).

7- It can have impacts on **viscosity** (Badro et al., 2003, Justo et al. 2015).

8- The transition can change **iron partitioning** (Burns, Cambridge Univ. Press, 1993). The **iron-free olivine** (forsterite) is **more viscous** than iron-bearing phases (Durham & Goetze, 1977; Durham et al., 1979), therefore an iron-free perovskite is likely to be **more viscous** than an iron-rich one.

Spin Transition in Ferropericlase

The influence of pressure, temperature and iron content on the spin transition

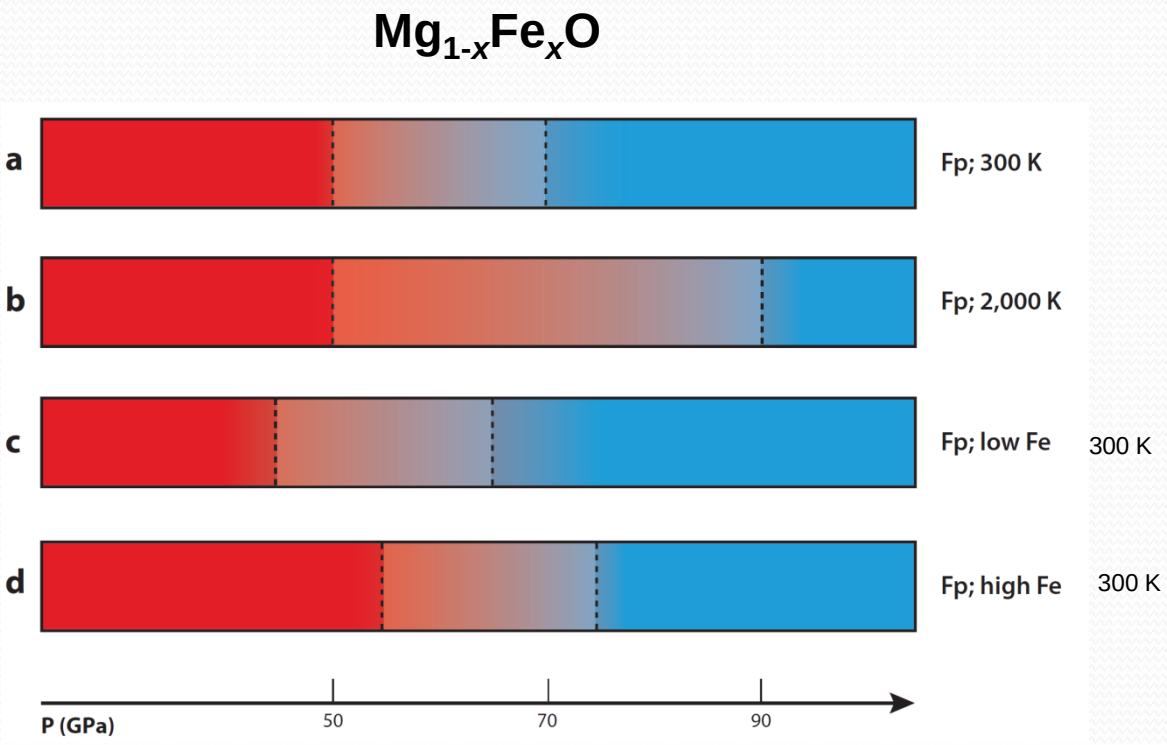

Schematic diagram of spin-state evolution in ferropericlase (Fp) as a function of pressure, temperature, and composition. Red denotes the high-spin state and blue the low-spin state (Badro 2014).

Spin Transition in Perovskite

Fe^{2+}- iron in $MgSio_3$-Pv is less likely to make transition to **LS**

Fe^{3+}- iron in $MgSio_3$-Pv occupies both **A** and **B** sites (with equal weighting)

Fe^{3+}- iron

A remains in **HS** in all mantle pressures

B → Fully **LS** in the range of 50-60 GPa

→ bulk modulus **hardening** **(Al-free)**

Adding Al:

a) increases the volume (the lattice) at low pressures (compared to Mg-endmember perovskite)

b) but Al-bearing perovskite is **more compressible**

→ bulk modulus **softening**

decrease in density Al-Pv ~ Mg-Pv at ~50 GPa

Catalli et al. (2009, 2010,2011)

$$\rho_K \sim \frac{1}{K_T}(P - P_r)$$

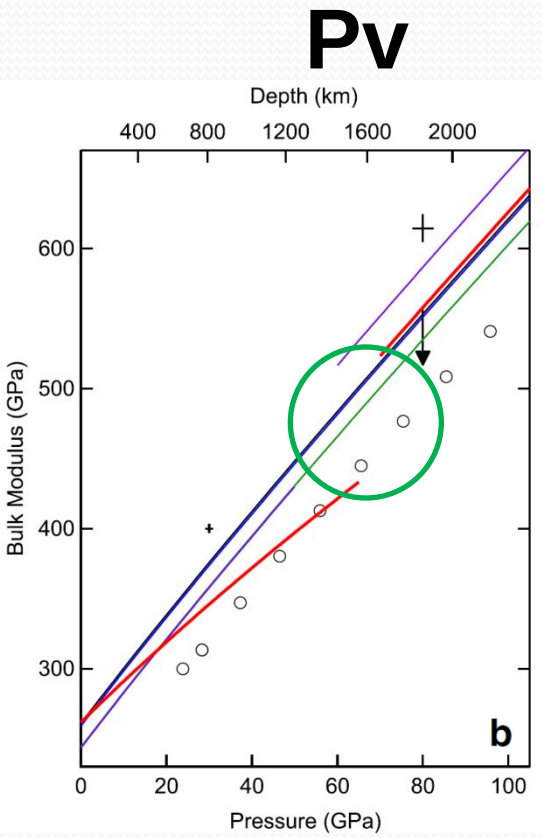

Spin Transition in Perovskite

The study of Ballaran et al. (2012) suggests that the impact of spin transition in Pv on the bulk modulus is **non-significant**.

However, there is **no experimental results** about the details of transition in the **MS-state.**

The Influence of Iron Spin Transition in Mantle Results from the Numerical Mantle Convection Models

Physical Properties Variations

Spin Crossover Transition in Ferropericlase

The volume of the mineral in the mixed state **MS** can be written as

$$V(n) = nV_{LS}(P,T) + (1-n)V_{HS}(P,T)$$

$n = 1$ *pure LS state*, $n = 0$ *pure HS state*

The thermal expansion coefficient of the **MS** state is by definition $\alpha(n) = \frac{1}{V(n)}\left(\frac{\partial V(n)}{\partial T}\right)_P$

Thus,

$$\alpha(n)V(n) = nV_{LS}\alpha_{LS} + (1-n)V_{HS}\alpha_{HS} + (V_{LS} - V_{HS})\left.\frac{\partial n}{\partial T}\right|_P$$

Also by definition $K_T(n) = -V(n)\left.\left(\frac{\partial P}{\partial V(n)}\right)\right|_T$

Then,

$$\frac{V(n)}{K_T(n)} = n\frac{V_{LS}}{K_{LS}^T} + (1-n)\frac{V_{HS}}{K_{HS}^T} - (V_{LS} - V_{HS})\left.\frac{\partial n}{\partial P}\right|_T$$

Note that for example :

$$\left(\frac{\partial(nV_{LS}(P,T))}{\partial T}\right)_P = n\left(\frac{\partial V_{LS}(P,T)}{\partial T}\right)_P + V_{LS}(P,T)\left(\frac{\partial n}{\partial T}\right)_P$$

Spin-induced Anomalies in Ferropericlase

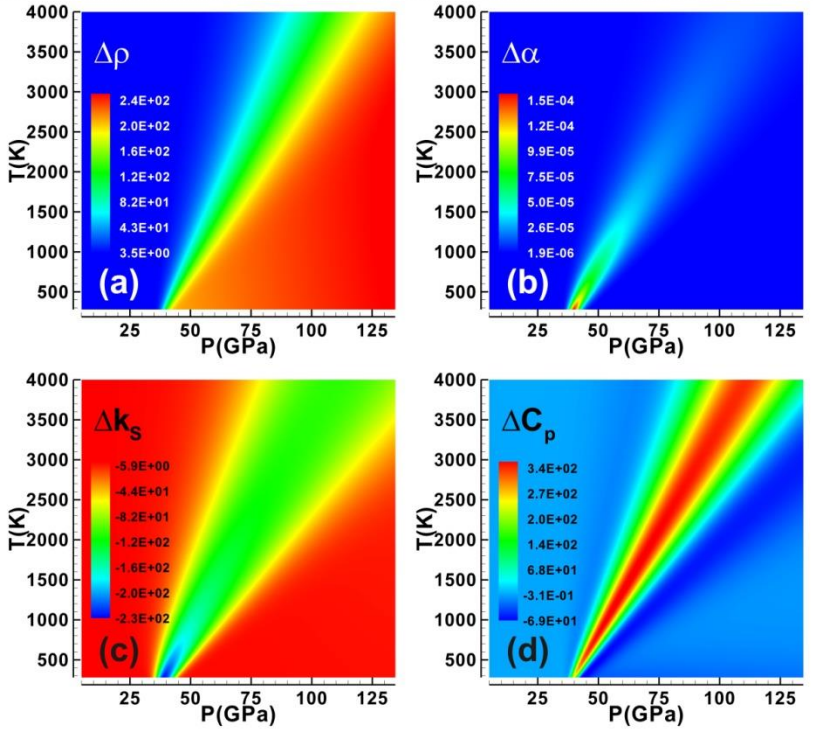

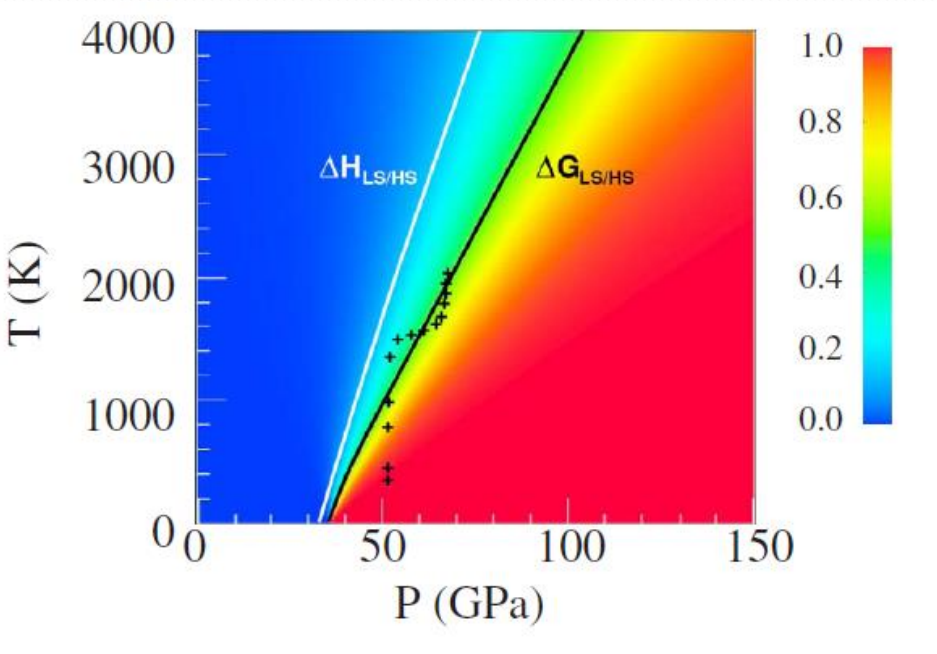

Spin States

Pressure and temperature dependence of spin-induced anomalies in **(a)** density in kg/m^3, **(b)** thermal expansivity in 1/K, **(c)** bulk modulus in GPa, and **(d)** heat capacity in J/kg/K in ferropericlase (Mg(1−x)FexO) with X = 0.1785. The anomalies are determined by the difference in thermodynamic properties between the mixed spin (MS) state and the HS state (Wu et al., 2009; Shahnas et al., 2011). The scale represents the depth in the mantle.

Physical Properties Variations

In the **MS region,** where **n** depends on the pressure and temperature, **the last terms** in these equations contribute **considerably** to the thermodynamic properties of the ferropericlase.

a) The **LS state has a smaller volume** than that of the **HS state**
b) n **decreases** with **temperature** and **increases** with **pressure**

Then
$\alpha(n)$ **increases** as HS → LS
$K(n)$ **decreases** as HS → LS

Spin Transition-Induced Anomalies

$$\rho = \rho_r[1 - \alpha(T - T_r)] + \frac{1}{K_T}(P - P_r) + \Delta\rho_i(\Gamma_i - \Gamma_{ri}) + \Delta\rho_{Tot}$$

$$\Delta\rho_\alpha = -\rho_r \Delta\alpha_s (T - T_r)$$

$$\Delta\rho_K = \rho_r \left[\left(\frac{1}{K_T + \Delta K_s} - \frac{1}{K_T}\right)(P - P_r)\right]$$

$$\Delta\rho_{Tot} = \Delta\rho_s + \Delta\rho_\alpha + \Delta\rho_K$$

Spin-induced Anomalies in Ferropericlase

Density Variation Due to the Spin Transition Induced Anomalies in the Thermal Expansivity and the Bulk Modulus

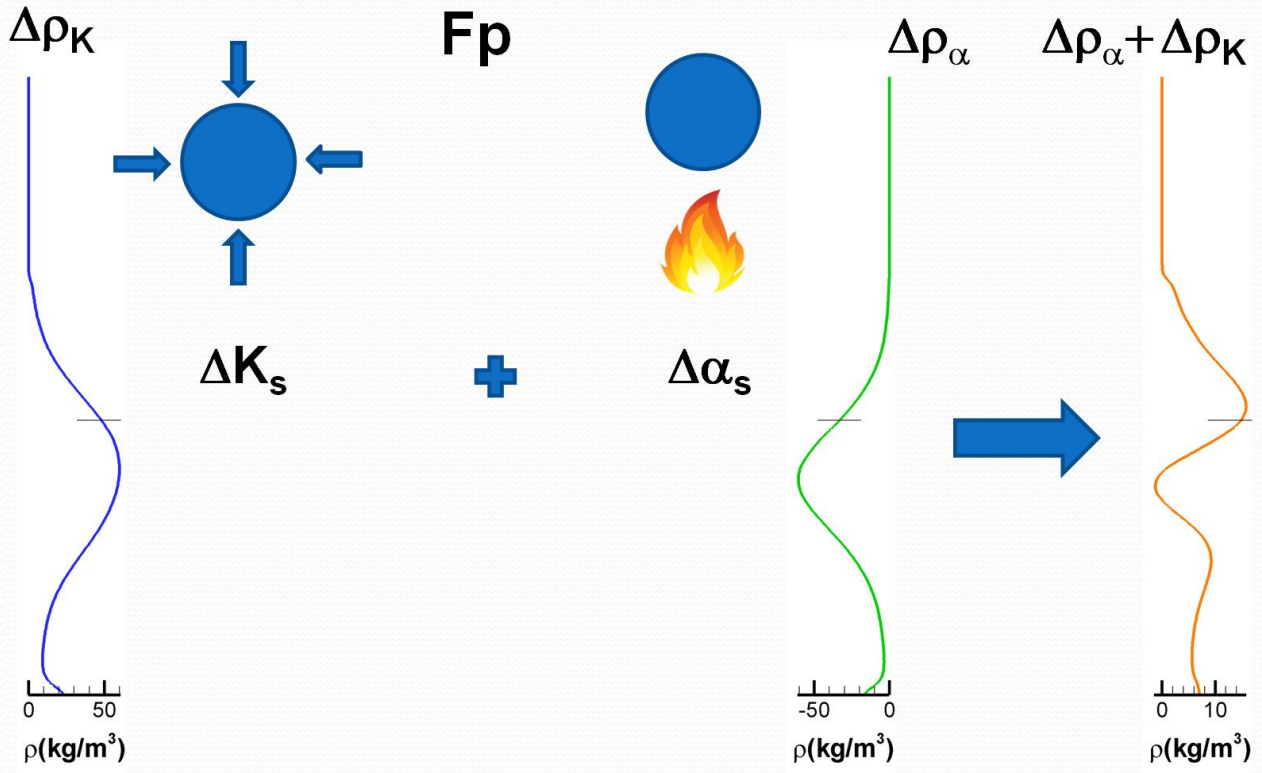

Spin-induced Anomalies in Ferropericlase

Density Variation in the Presence of Iron Spin Transition

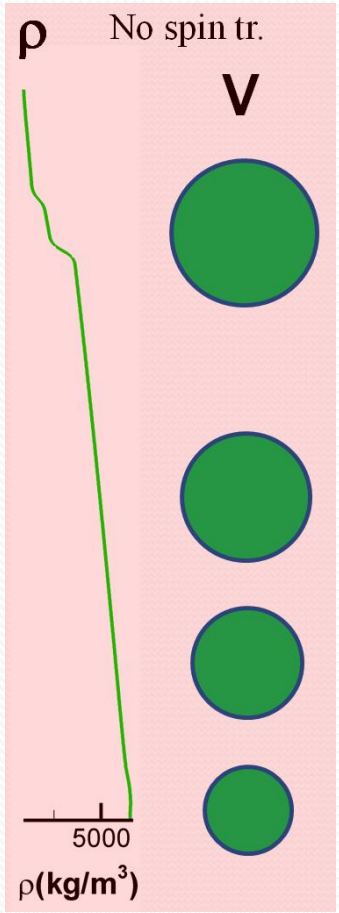

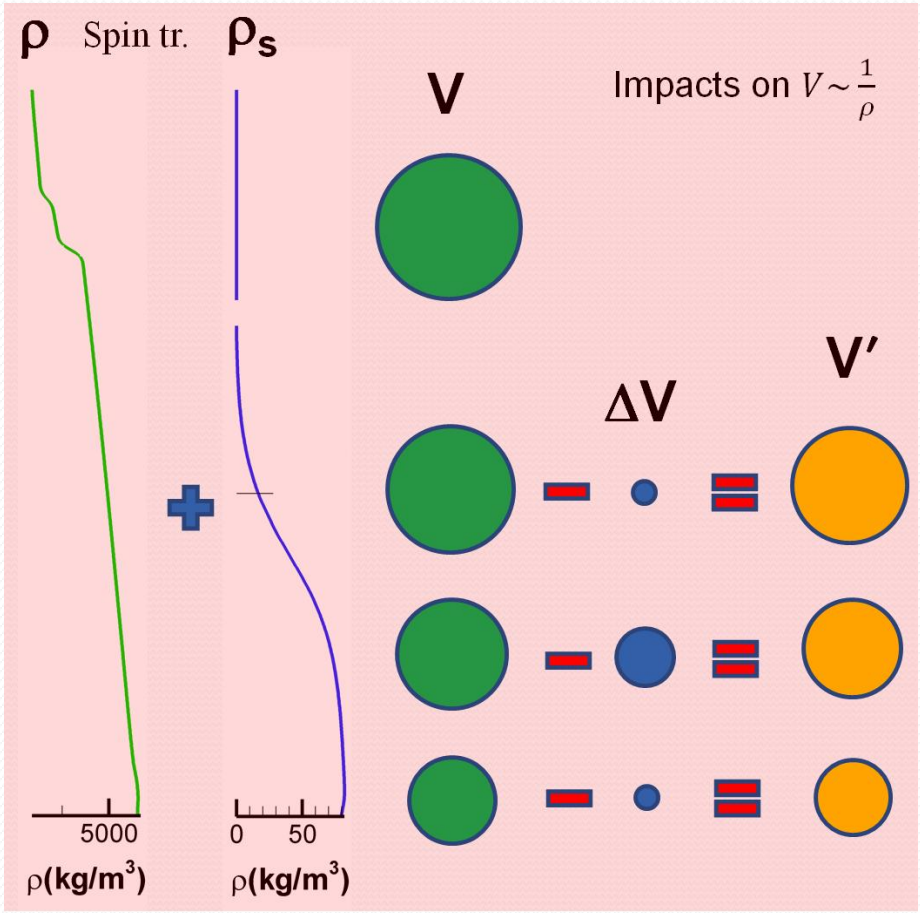

Spin-induced Anomalies in Fp

Density Anomalies in Fp

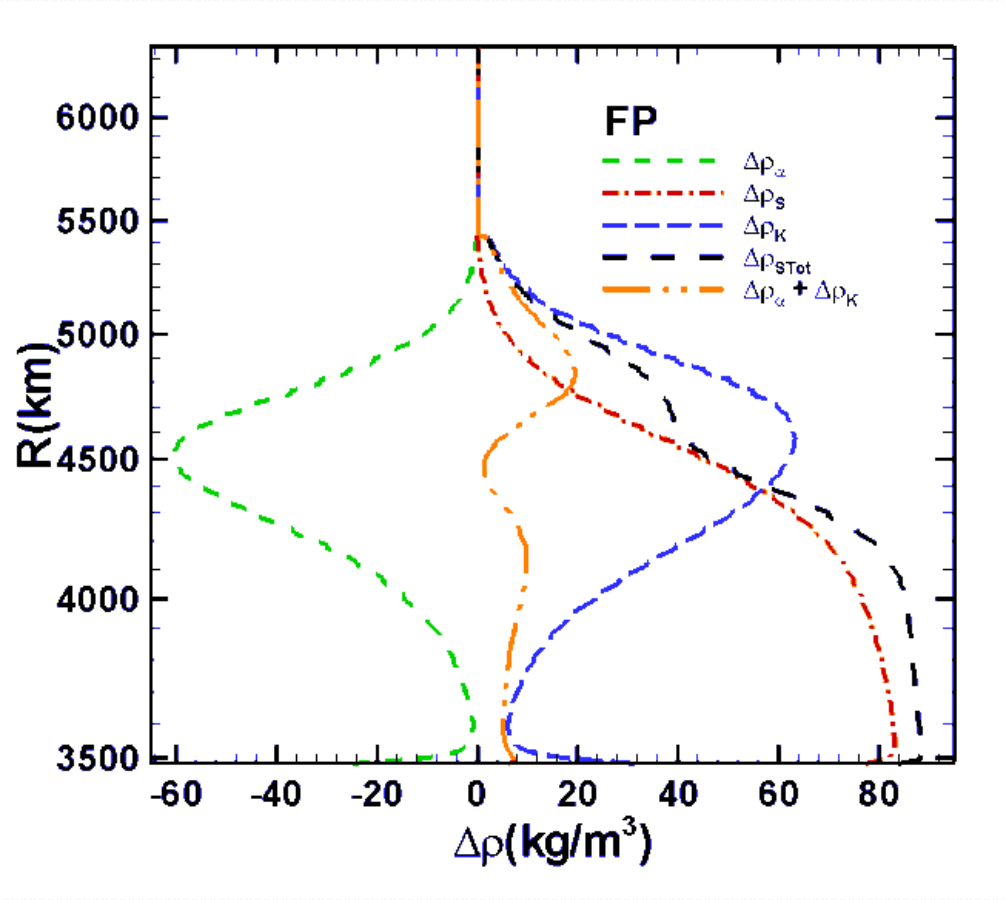

$$\Delta\rho_{STot} = \Delta\rho_s + \Delta\rho_\alpha + \Delta\rho_K$$

Iron Spin Transition in Fp

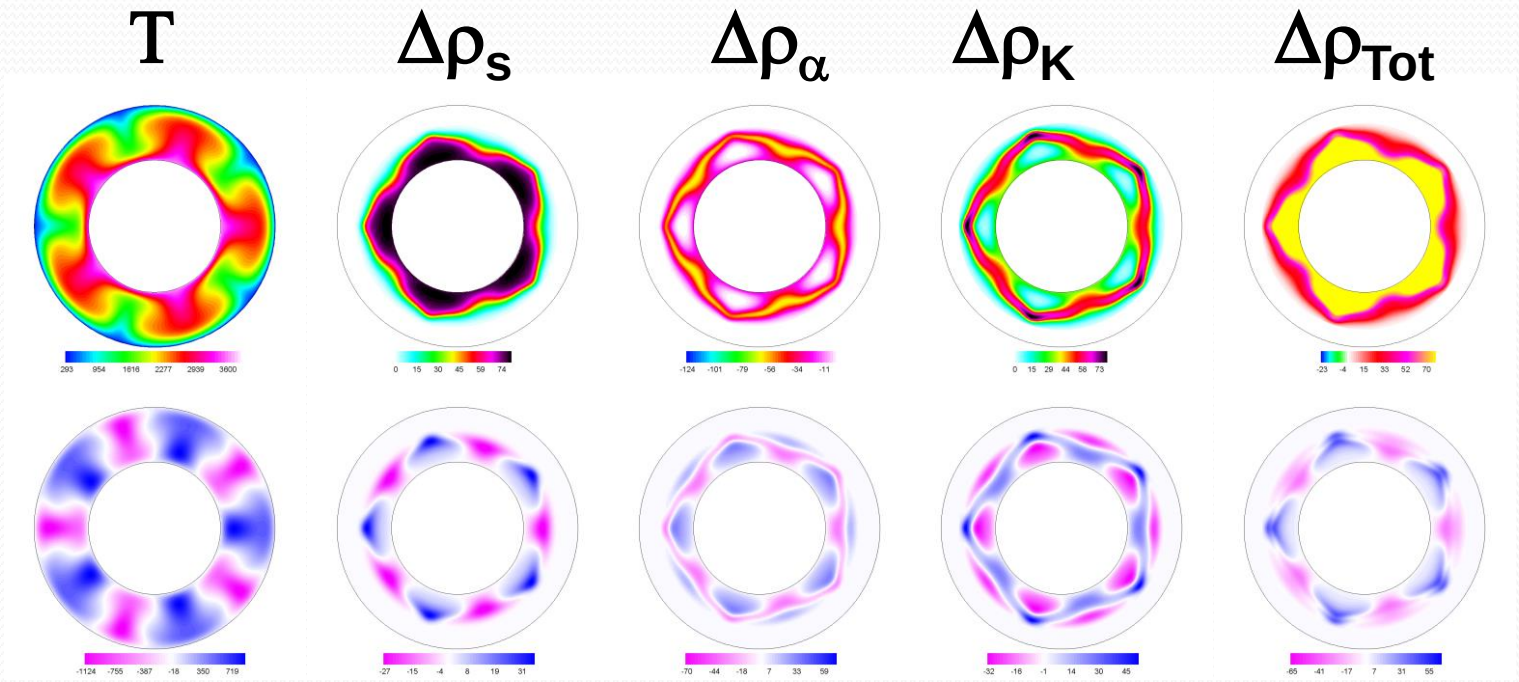

$q - q_{ave}$

Test models

Spin-induced Anomalies in Fp+ Pv

Density Anomalies in Fp + Pv, Assuming Different Degrees of Bulk Modulus Hardening in Pv.

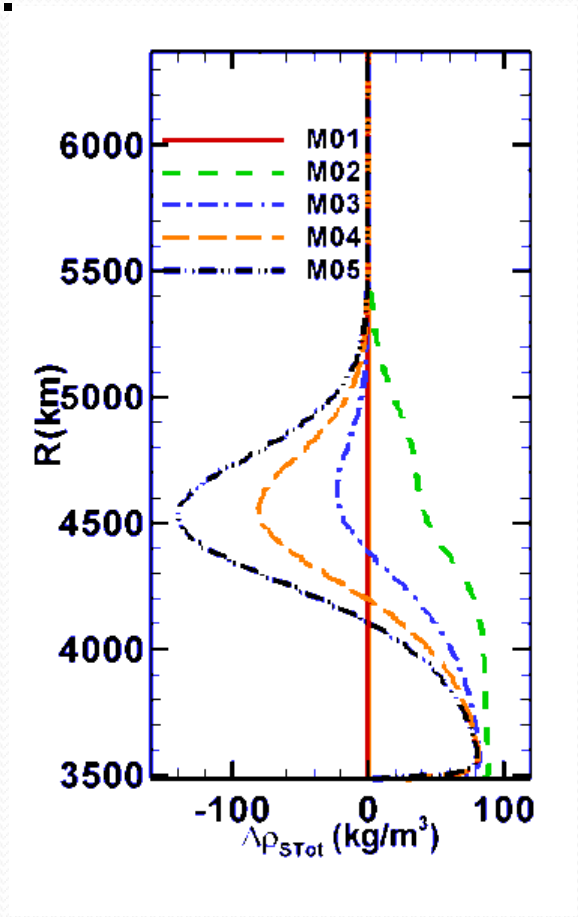

$\Delta\boldsymbol{\rho}_{\boldsymbol{Tot}}$

Iron Spin Transition in Fp + Pv

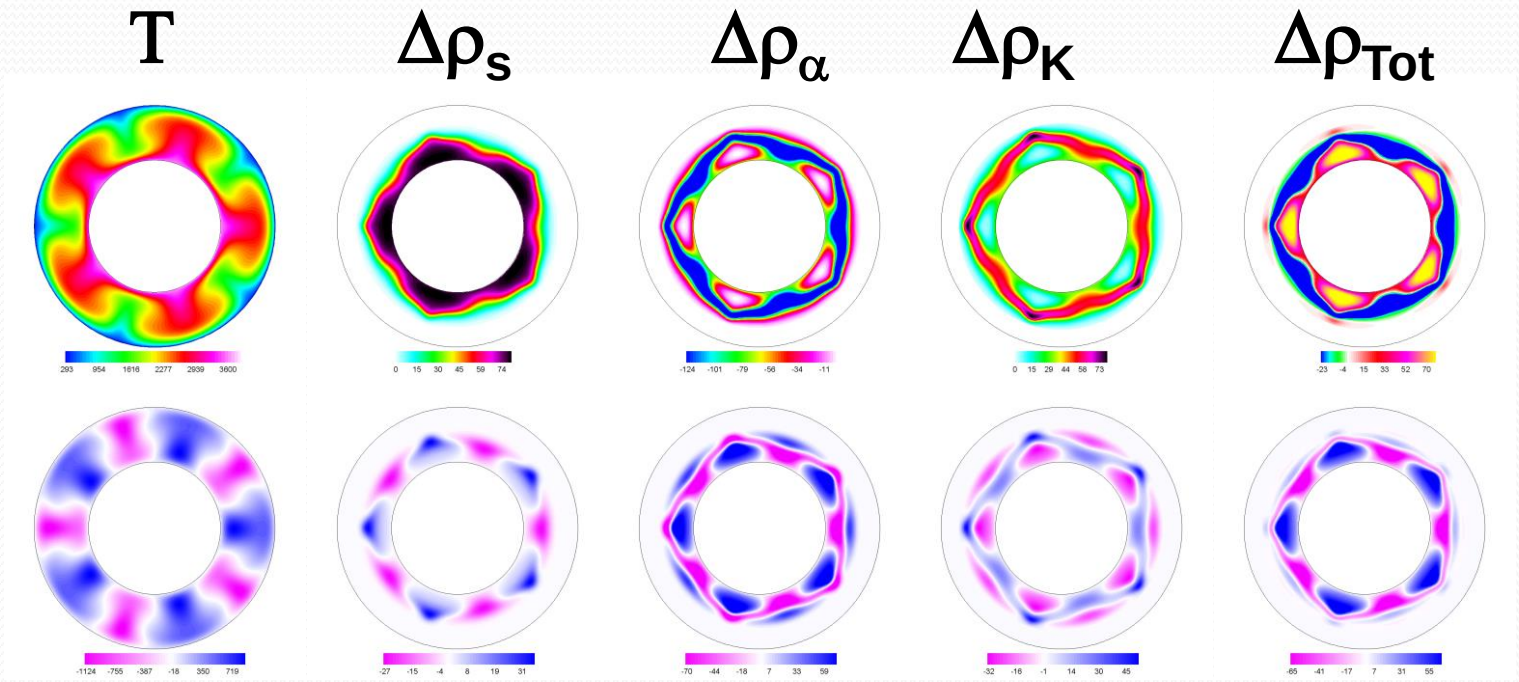

$q - q_{ave}$

Test models

(Shahnas et al., 2017, EPSL)

Evidences for Mid-Mantle Flow Stagnations

Seismic Scatterers in the Mid-Lower Mantle

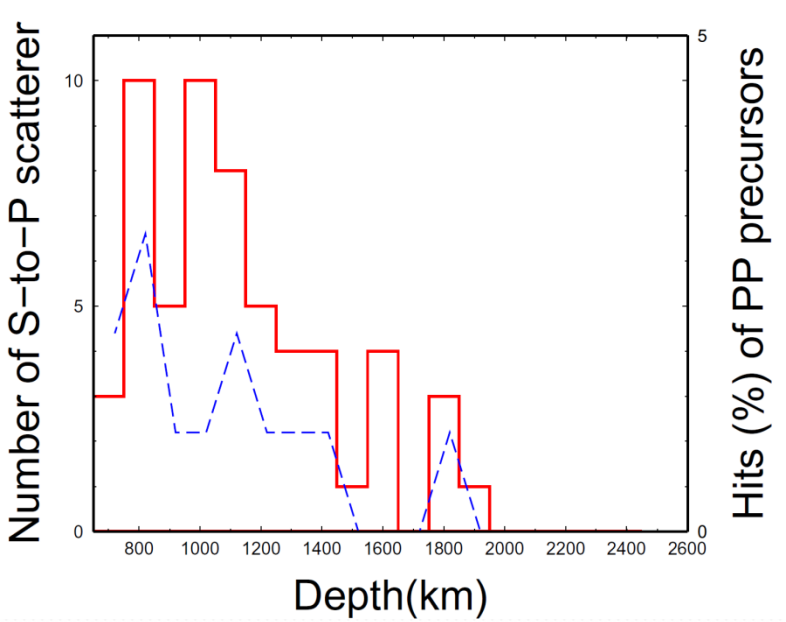

Kaneshima (2016)

Red line shows the histogram of the number of mid-lower mantle S-to-P scatterers in the **western Pacific** as a function of depth (Kaneshima and Helffrich, 2010; Kaneshima, 2003; Kaneshima, 2009; Kaneshima, 2013; Li and Yuen, 2014; Niu, 2014; Vanacore et al., 2006; Yang and He, 2015).

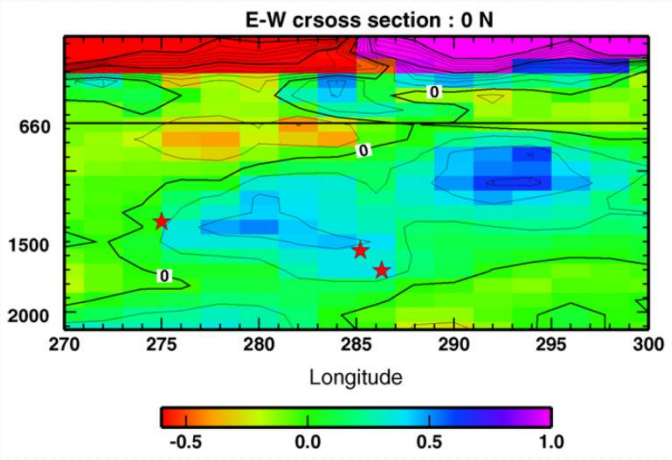

South America

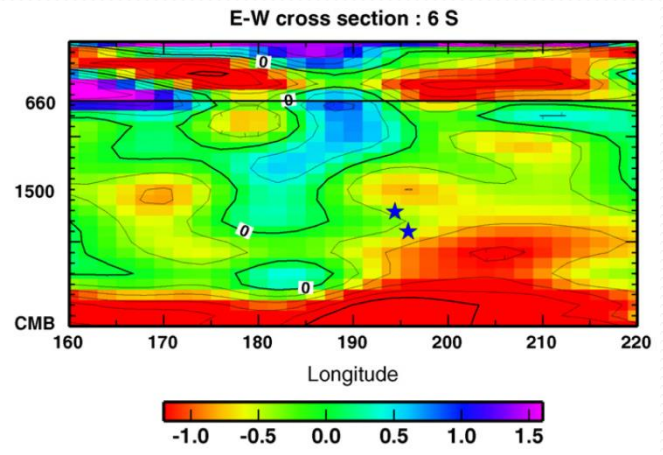

Fiji

Kaneshima and Helffrich (2010)

Spin-Induced Mid-Mantle Stagnation

Lower mantle thermal anomalies below India and Tibet were expected to have been recycled to the bottom of mantle until now. However, tomographic imaging reveals the existence of fossil thermal anomalies in these regions.

Something should have delayed this journey. Spin transition?

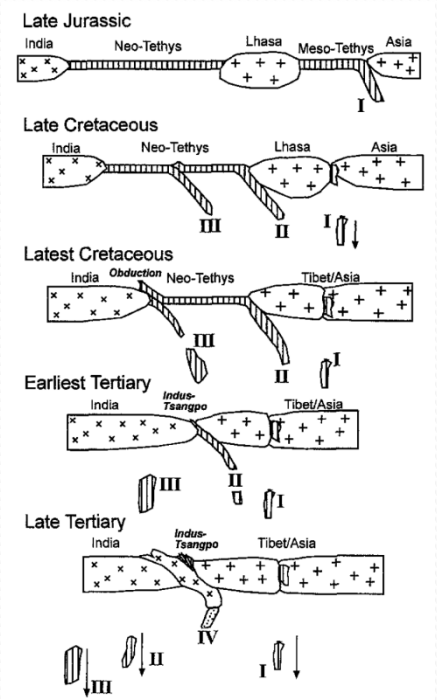

163-145 Ma

100-66 Ma

66-2.5 Ma

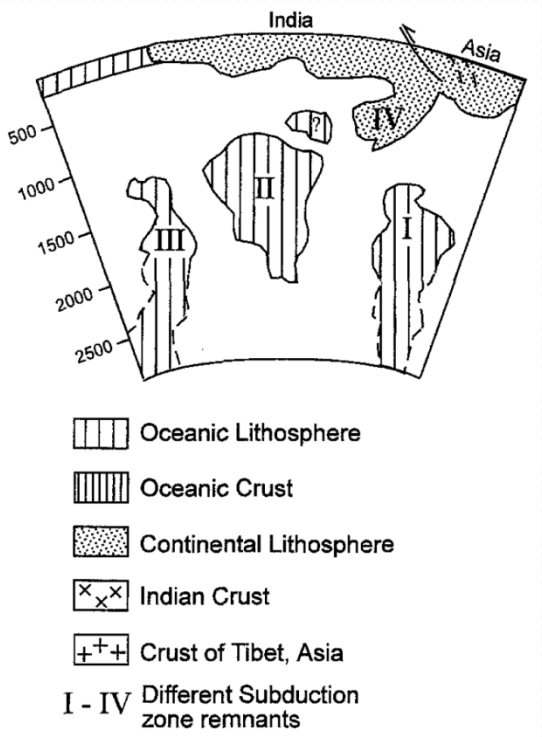

Cartoon depicting the evolution of Mesozoic Tethyan subduction zones.
Lower mantle thermal anomalies that have been imaged tomographically below India and Tibet (Van der Voo et al., 1999).

Impacts of the Iron Spin Transition in the Lower Mantle Material Properties

Theoretical Studies

Temperature and Pressure Dependence of Viscosity

Activation Energy

In chemistry and physics, activation energy is the minimum amount of energy that must be provided for compounds to result in a chemical reaction **(joules per mole (J/mol)).**

Arrhenius equation

The Arrhenius equation is a relationship between the activation energy and the rate at which a reaction proceeds.

$$k = Ae^{-E_a/RT}$$

$R = 8.31446261815324$ *(J/K/mol) (Gas constant)*

E_a: *Activation energy (J/mol)*

T: *Temperature (K)*

A: *Factor*

Higher temperature (T) and **lower** activation energy (E_a) → **speed up a reaction**

Temperature and Pressure Dependence of Viscosity

Viscosity - Arrhenius-Like

Viscosity generally becomes smaller as temperature is elevated. As the temperature increases the enhancement in kinetic motion promotes the breaking of intermolecular bonds. A simple model assumes that the viscosity obeys an **Arrhenius-like** equation of the form:

$$\eta = \eta_0 e^{+E_a/RT}$$

Higher temperature (T) and **lower** activation energy (E_a) → **lower viscosity**

Adjustment

In order to adjust the viscosity model to a defined viscosity at a certain depth, we can write the viscosity relation as:

$$\eta(z) = \eta(z_0) e^{\left(\frac{E_a(z)}{RT(z)} - \frac{E_a(z_0)}{RT(z_0)}\right)}$$

Note that the activation energy can change by the **elastic properties** and **depth**.

Temperature and Pressure Dependence of Viscosity

Adiabatic Temperature Gradient

An adiabatic temperature gradient is the temperature gradient resulting from isentropic pressure changes.

$$\nabla T_S \equiv \frac{\alpha T}{\rho c_P} \nabla P$$ *Adiabatic temperature gradient*

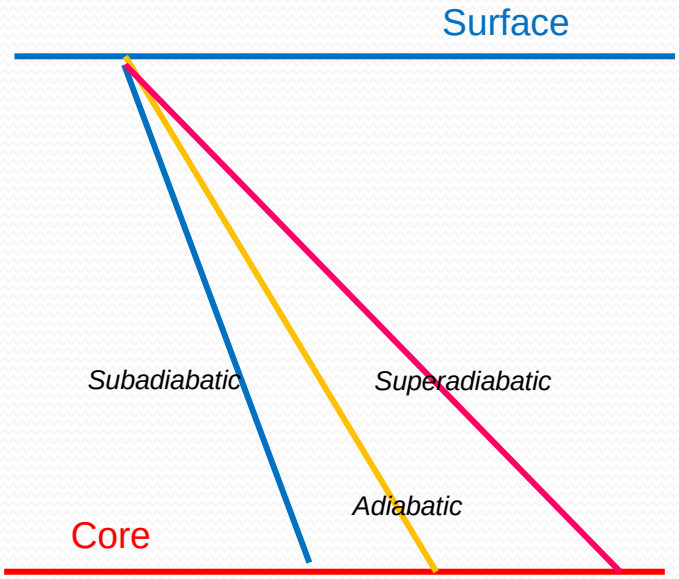

Spin Transition: Impacts on the Viscosity

Double Pick Viscosity Model of Mantle

Some previous studies suggest a viscosity model with two picks in the lower mantle (Mitrovica and Forte (2004).

In a theoretical study Justo et al. (2015) attempt to explain the double pick viscosity model of the mantle (Mitrovica and Forte (2004) as a consequence of spin transition in the lower mantle minerals.

The viscosity is given by:

$$\eta(z) = \eta(z_0) e^{\left(\frac{G^*(z)}{RT(z)} - \frac{G^*(z_0)}{RT(z_0)}\right)}$$ *Thermally activated process*

$R = N_A K$ *Gas cont.*

$N_A = 6.02214076 \times 10^{23}\ mol^{-1}$ *Avogadro cont.*

$K = 1.380649 \times 10^{-23}\ J/K$ *Boltzmann const*

Spin Transition: Impacts on the Viscosity

The activation energy $G^*(z)$ can be described as a linear combination of energies from **pure shear**, $G{*}s(z)$, and **pure dilatation**, $G^*_D(z)$, mechanisms:

$$\boldsymbol{G^*(z) = \delta G_S^*(z) + (1-\delta) G_D^*(z)}$$

and can be calculated from:

$$\frac{\boldsymbol{G_S^*(z)}}{\boldsymbol{G_S^*(z_0)}} = \left[\frac{V_S(z)}{V_S(z_0)}\right]^2$$

and

$$\frac{\boldsymbol{G_D^*(z)}}{\boldsymbol{G_D^*(z_0)}} = \left[\frac{V_\phi(z)}{V_\phi(z_0)}\right]^2$$

G: *Activation energy*

$0 \leq \delta \leq 1$

$\eta(z_0) = 1.14 \times 10^{21}$ Pa.s,

$z_0 = 660\ km\ depth$

$V_S = \sqrt{\frac{\mu}{\rho}}$ Shear velocity

$V_\phi = \sqrt{\frac{K}{\rho}}$ Bulk velocity

Spin Transition - Bulk Modulus Softening

Spin transition influences the bulk modulus, density and bulk velocity.

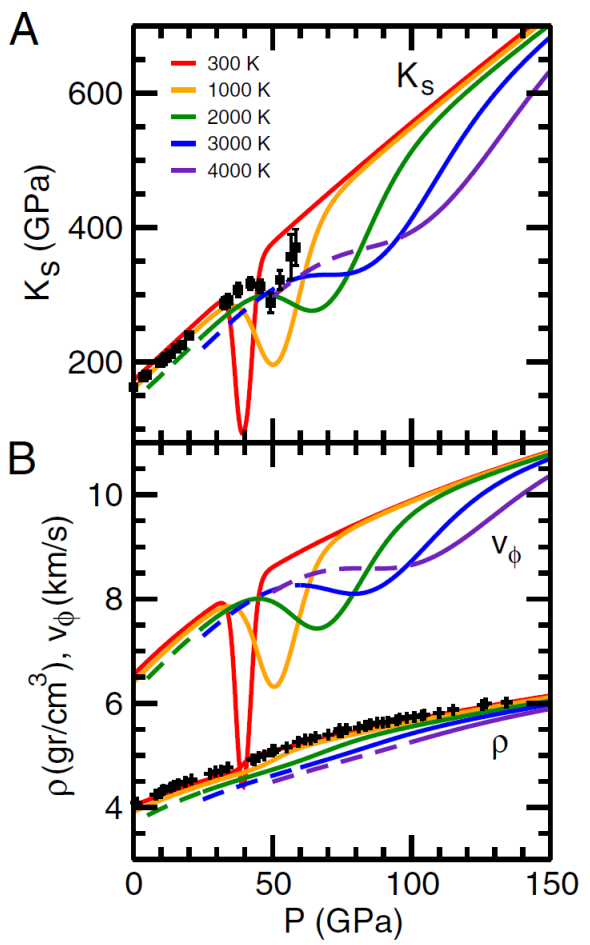

Ferropericlase $Mg_{1-x}Fe_xO$ (x=0.1875)

This cross-over has important consequences for elasticity such as an anomalous **bulk modulus (K_S)** reduction.

$$\rho_K \sim \frac{1}{K_T}(P - P_r)$$

$$V_\phi = \sqrt{V_p^2 + \frac{4}{3}V_s^2}$$

Pressure dependence of the calculated

A) adiabatic bulk modulus K_S, and

B) bulk wave velocity V_ϕ and density,ρ of $Mg_{1-x}Fe_xO$ (x=0.1875) along several isotherms (Wentzcovitch et al., 2009) **assuming spin transition in Fp.**

Spin Transition: Impacts on the Viscosity

Normalized Fp viscosity as a function of depth for (a) **adiabatic** and (b) **superadiabatic** geotherms for several contributions of dilatation and shear mechanisms compared with mantle viscosity model of Mitrovica and Forte (2004) (gray line). δ = 0 pure dilatation, Justo et al. (2015).

Ferropericlase $Mg_{1-x}Fe_xO$ (x=0.1875)

The red, orange and green lines represent respectively δ =0 (pure dilatation), δ =0.5, and δ =1.0 (pure shear). Here, $G^*(z_0)$ =300kJ/mol and the fluid is considered Newtonian (n =1).

$\sigma \sim \dot{\varepsilon}$ Newtonian Fluid

Spin transition influences V_S and V_S and hence $G_S{}^*$ and $G_D{}^*$ and therefore η

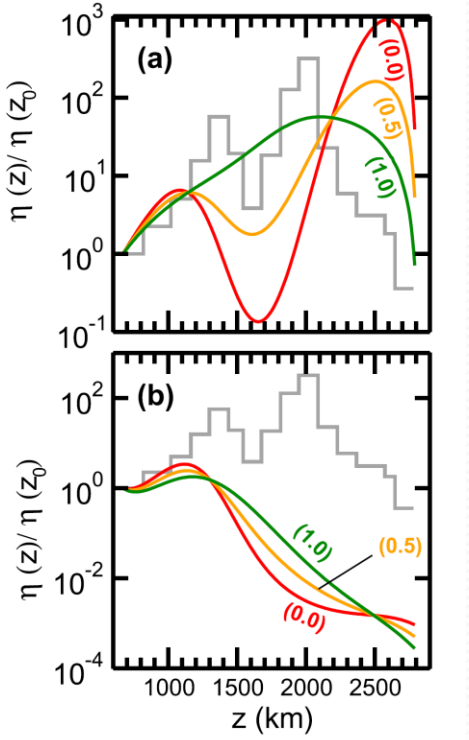

a) For adiabatic geotherm
b) For superadiabatic geotherm

Numerical Convection Models

Results From Numerical Convection Models

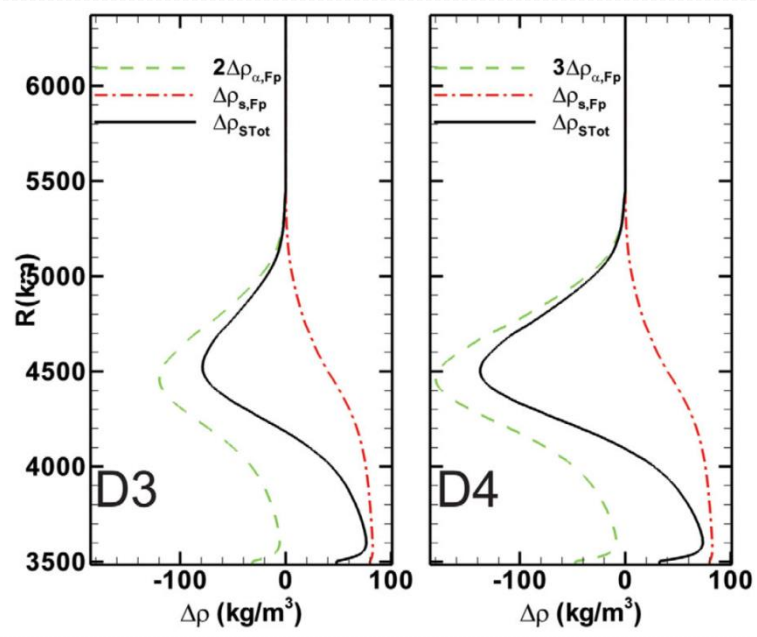

Spin transition-induced density anomaly models employed in our numerical convection models.

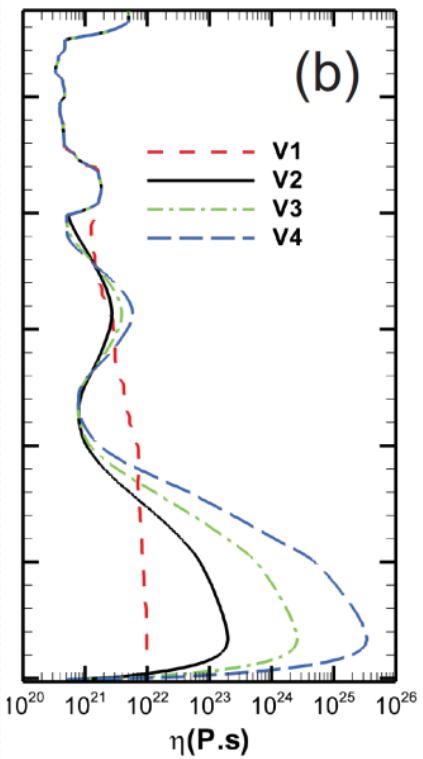

Double-pick viscosity models:
V1=VM3 depth-dependent viscosity
V2-V4=VMPT2-VMPT4 spin transition-induced viscosity models (Shahnas et al., 2017).

Numerical Convection Models
Spin Transition Induced Superplumes

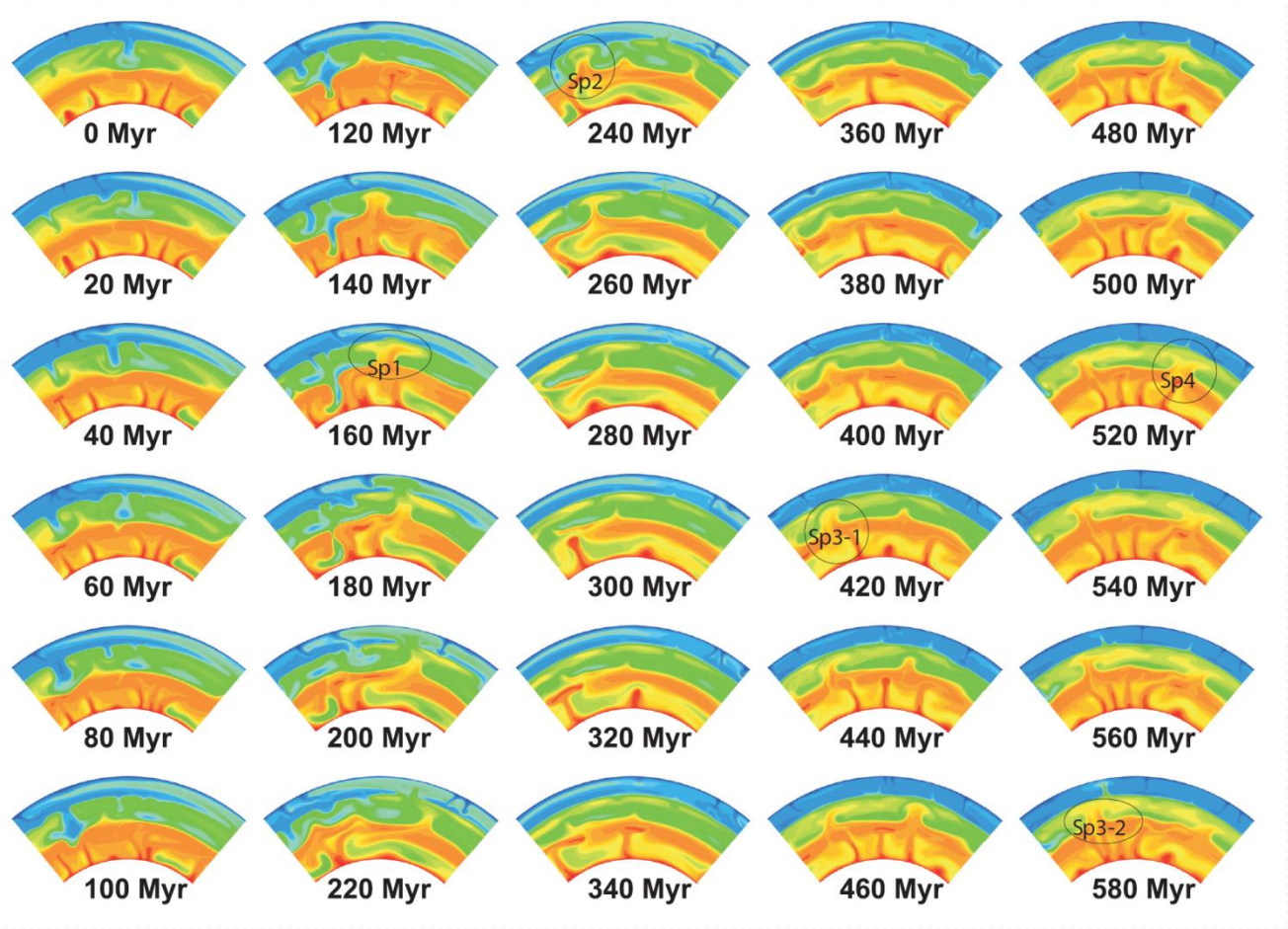

Temperature fields for model V2D4 with (P,T)-dependent viscosity model (Shahnas et al., 2016)

Numerical Convection Models
Spin Transition Induced Superplumes

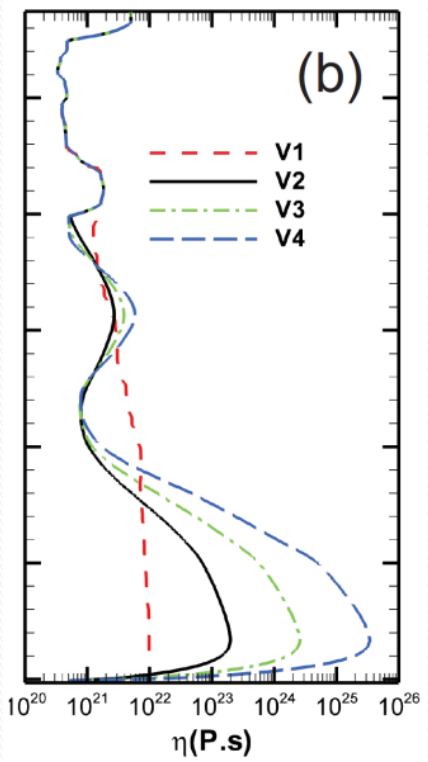

Double-pick viscosity models:
V1=VM3 depth-dependent viscosity
V2-V4=VMPT2-VMPT4 spin transition-induced viscosity models (Shahnas et al., 2017).

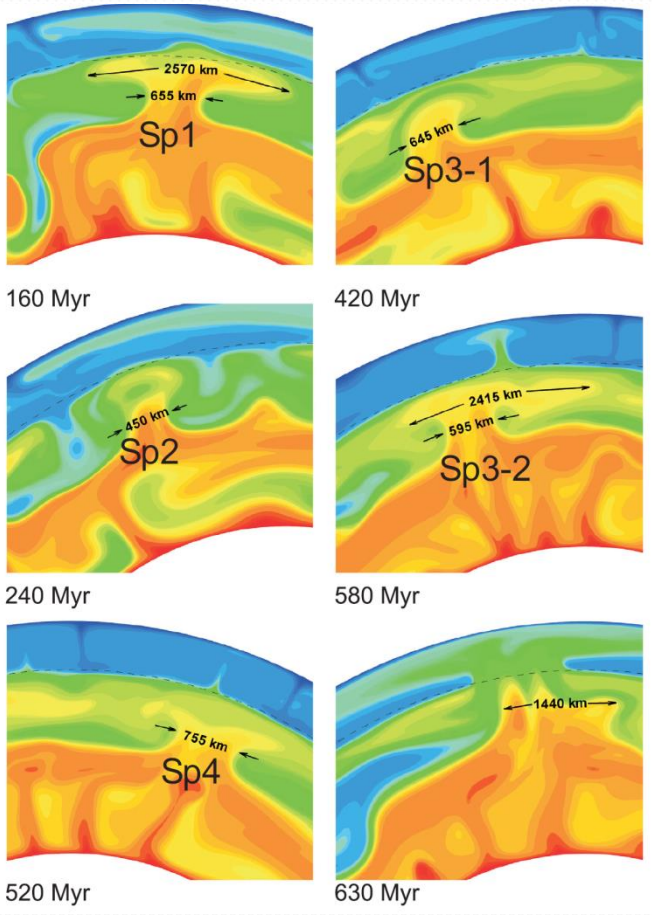

Close-up of the snapshots indicated in the previous slide

Numerical Convection Models

Spin Transition Induced Superplumes

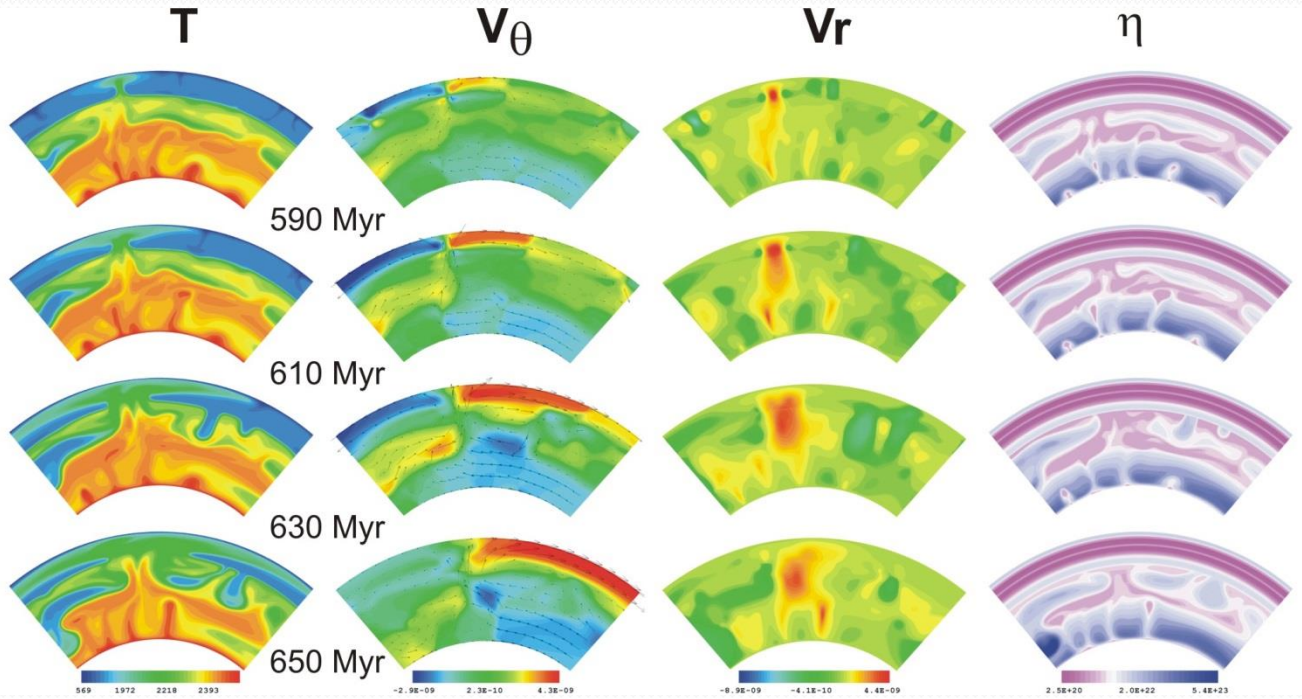

Temperature (K), lateral velocity (m/s), radial velocity (m/s) and viscosity (Pa.s) fields (from left to right) of the model **V2D4** for 60 Myr evolution. Velocity arrows are superimposed over the lateral velocity fields. The flow velocity at the surface due to the influence of this superplume reaches up to ~16 cm/yr. The shear stress at a depth of 30 km at the top of plume reaches ~43 Mpa (Shahnas et al., 2016).

Numerical Convection Models
Mid-Mantle Stagnation

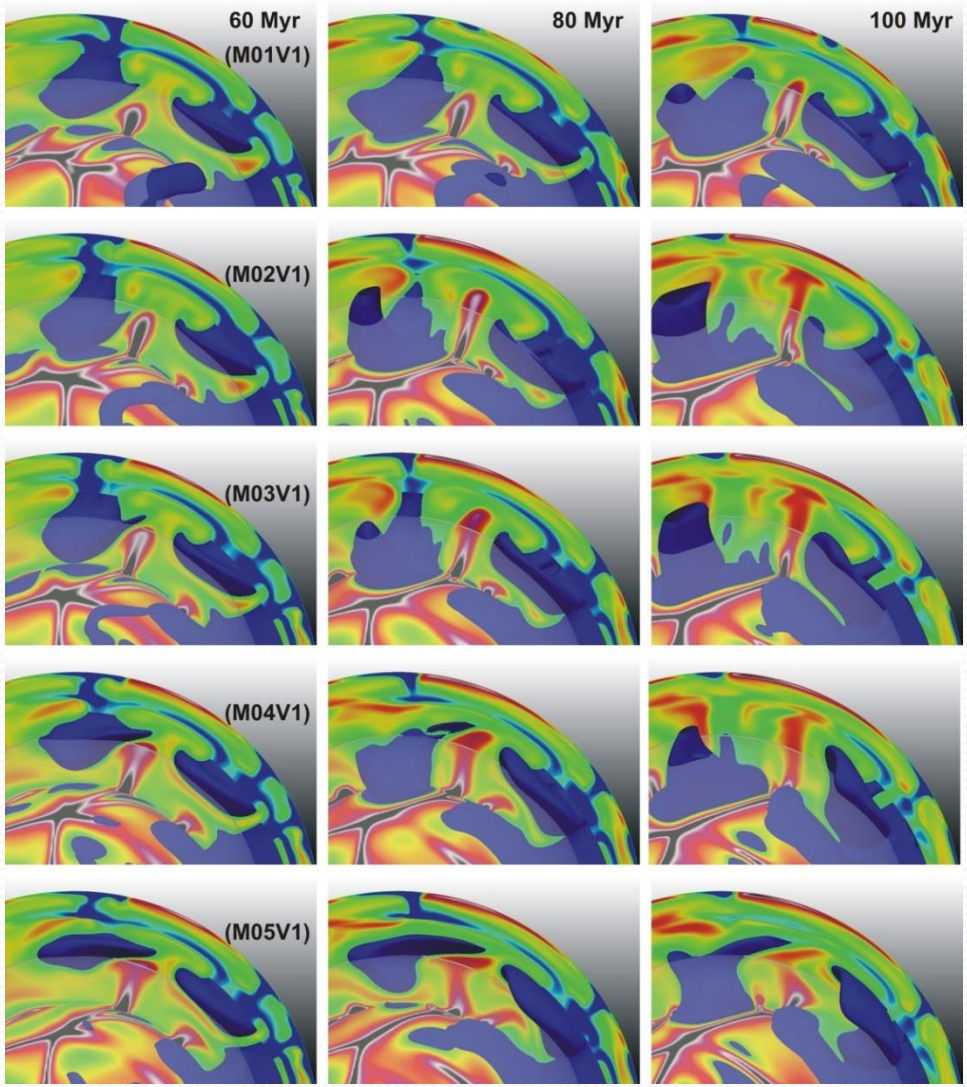

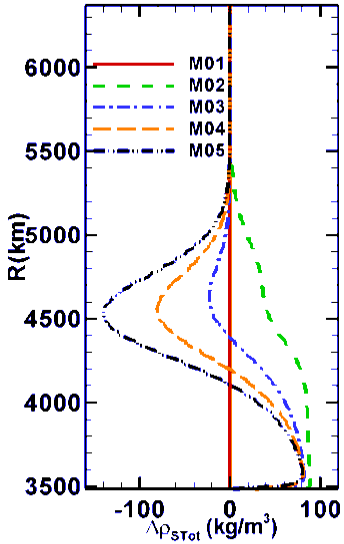

$$2 \times \theta \times \phi \times r = 2 \times 130 \times 360 \times 201$$

Snapshots of five models:
M01V1) no spin transition,
M02V1) with spin transition in Fp,
M03V1) with spin transition in Fp+Pv
M04V1) the same as M03V1 but with stronger effect from the Pv-phase
M05V1) the same as M03V1 but more stronger effect from the Pv-phase
(Shahnas et al., 2017, EPSL)

Spin-Induced Source Isolation

Alternative Explanation for MORB and OIB

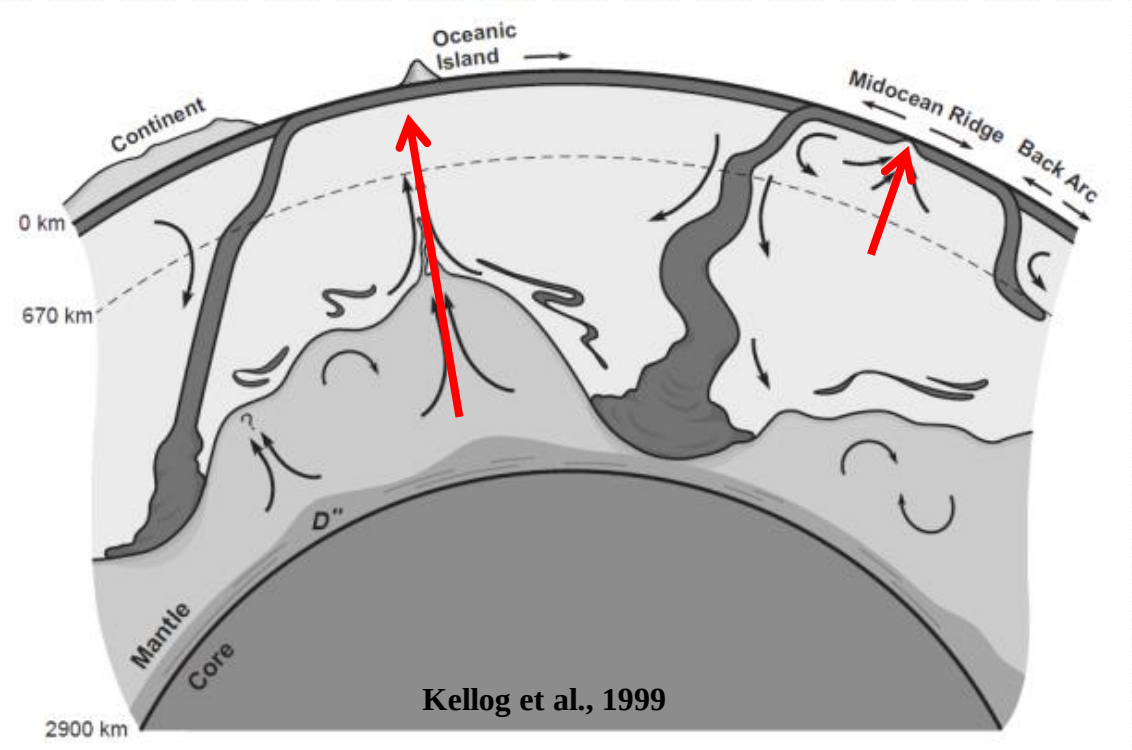

Kellog et al., 1999

Spin-induced process may also provide an alternative explanation for the mid-ocean ridge basalts (MORB) and oceanic island basalts OIB) source isolation.